THESIS

THE ABUNDANCE AND SOURCES OF ICE NUCLEATING PARTICLES (INPS) WITHIN ALASKAN ICE FOG

Submitted by

Emily Lill

Department of Atmospheric Science

In partial fulfillment of the requirements

For the Degree of Master of Science

Colorado State University

Fort Collins, Colorado

Spring 2024

Master's Committee:

Advisor: Emily V. Fischer
Co-Advisor: Jessie Creamean

Sonia Kreidenweis
Diana Wall

ABSTRACT

THE ABUNDANCE AND SOURCES OF ICE NUCLEATING PARTICLES (INPS) WITHIN ALASKAN ICE FOG

Fairbanks, Alaska often experiences low visibility due to air pollution. Low wind speeds and strong temperature inversions paired with local emissions from the burning of wood, oil, gasoline, and coal lead to wintertime pollution events where concentrations of fine particulate matter ($PM_{2.5}$) often reach 50 g m^{-3}, exceeding the Environmental Protection Agency (EPA) 24-hour National Ambient Air Quality Standard (NAAQS) of 35 g m^{-3}. When temperatures fall below -15°C and sufficient moisture is present, these pollution events can facilitate the formation of ice fog, further worsening air quality and visibility issues for aviation and transportation. The formation of ice crystals from supercooled droplets is aided by a small, but critical, number of aerosol particles that potentially act as ice nucleating particles (INPs). However, studies evaluating the quantities and sources of INPs during ice fog are limited. The Alaskan Layered Pollution and Chemical Analysis (ALPACA) field campaign included deployment of a suite of atmospheric measurements in January - February 2022 with the goal of better understanding atmospheric processes and pollution under cold and dark conditions. We report on measurements of particle composition, particle size, INP composition, and INP size during an ice fog period (29 January - 3 February). There was a 153% increase in coarse particulate matter (PM_{10}) during the ice fog period, associated with a decrease in air temperature. Results also show a 58% decrease in INPs active at -15°C during the ice fog period, indicating that particles were scavenged by ice fog ice crystals, likely via nucleation. Peroxide and heat treatments were performed on INPs in order to determine the fraction of INPs that were biological, organic, or inorganic. One hypothesis consistent with the results of the peroxide treatments is that more efficient INPs derived from biological materials or organics that typically activate at warmer freezing temperatures may have been depleted during the ice fog event. The

reduction in heat-labile INPs during the ice fog event was unexpected for Fairbanks in the winter due to the very low temperatures and limited biological aerosol sources. Aerosol compositional measurements corroborate the presence of INPs from biomass burning and road dust.

ACKNOWLEDGEMENTS

I would like to thank my advisors, Dr. Emily Fischer and Dr. Jessie Creamean for guiding and supporting me throughout my master's degree. Emily has been a fantastic mentor to me since I was her undergraduate intern. She saw potential in me that I didn't see myself and has pushed me to become the best scientist (and person) I could be. Jessie truly took me under her wing and fostered my love of fieldwork. She made sure that my time spent in the Alaskan winter was not only a valuable learning experience, but also a fun one. A huge thank you to Paul DeMott, Russell Perkins, and Ezra Levin for all their help and support in the field. I would also like to thank Dr. Sonia Kreidenweis and Dr. Diana Wall for serving on my committee.

A huge thank you to the Fischer group: Julieta Juncosa Calahorrano, Kimberley Corwin, Madison Shogrin, Olivia Sablan, En Li, Lena Low, Daniela Guevara, and Jennifer McGinnis for creating such a great community. Another thank you to so many other graduate students at CSU Atmospheric Science who have supported me and become great friends. Lastly, I would like to thank my family for supporting and encouraging me throughout my life to go out and pursue my dreams. I would not be where I am today without them.

This work was supported by the National Science Foundation (NSF) grant number AGS-2037119

TABLE OF CONTENTS

Chapter 1

INTRODUCTION

Air pollution is an emerging issue for the Arctic with major contributions from both local and remote sources (Law and Stohl, 2007). The Arctic is often impacted by pollutants transported from North America, Asia, and Europe, specifically in the winter during the so-called Arctic haze (Law et al., 2014). In the summertime, wildfire smoke from both local and long-range sources can negatively impact Arctic air quality (Simpson et al., 2011; Woo et al., 2020). In the winter, strong inversions can trap and lead to the accumulation of pollution (Schmale et al., 2018). Industrial development is expected to increase in the Arctic due to warming temperatures, creating opportunities for economic growth and a growing population (Fondahl and Larsen, 2015). Additionally, warming temperatures are predicted to lead to an increase in biogenic volatile organic compound (VOC) emissions (Kramshøj et al., 2016) and emissions from activities such as gas flaring due to the projected increased industrial development (Li et al., 2016). These conditions are likely to lead to worsening air quality (Law et al., 2017).

Air pollution in the Arctic is often concentrated by both topography and meteorology. In the winter, the Arctic experiences a lack of solar heating because there are only a few hours of daylight coupled with a high surface albedo from the heavy snowpack (Joyce et al., 2014). The lack of solar heating suppresses vertical convective mixing, which can lead to strong surface-based inversions (Wendler and Jayaweera, 1972). These surface-based inversions occur quite frequently, about 50% of the time from November to March in Fairbanks, Alaska (Tran and Mölders, 2011; Cesler-Maloney et al., 2022). Figure 1.1 demonstrates how strong inversions are correlated with low solar radiation. Fairbanks is surrounded by mountains which shelter it from winds (Willis and Grice, 1977). The combination of a strong inversion and weak winds create an environment with little dispersion where pollutants can accumulate.

In the Arctic, ice fog is classified as pollution and its formation exacerbates visibility challenges. When temperatures fall below -15°C, high levels of pollution can lead to the formation of ice

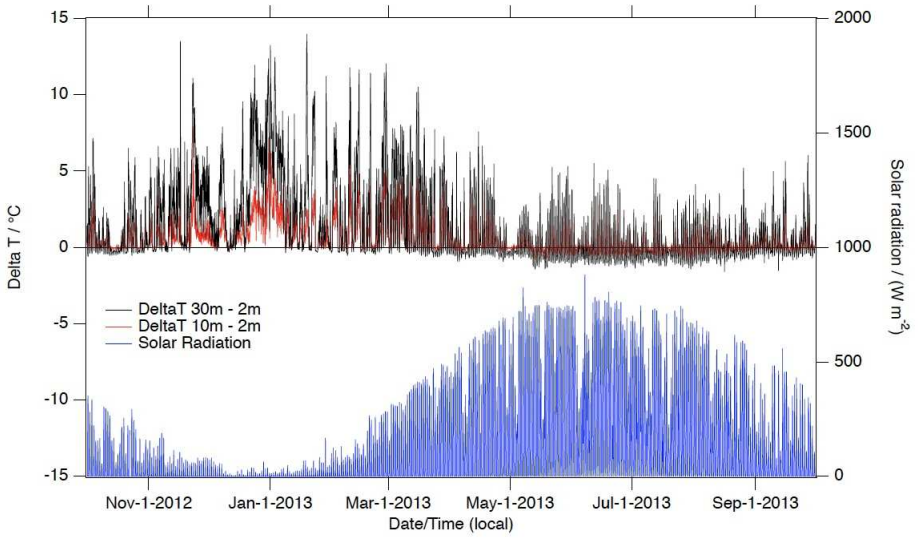

Figure 1.1: Temperatures at 2, 10, and 30 meters above ground level and incoming solar radiation measured on a meteorological tower measured from the valley floor in Fairbanks, Alaska by Simpson et al. (2019).

fog, which can worsen visibility issues for transportation (Gultepe et al., 2017). Those living in communities affected by ice fog often experience issues with aviation due to poor visibility and aircraft icing (Gultepe et al., 2014). This is a major hindrance for communities that do not have access to highways as they depend on air travel for essential services and supplies. Ice fogs often coincide with extreme pollution events leading to the presence of both non-activated, interstitial aerosols and particles from the ice fog itself (Robinson et al., 1957). Fairbanks is a unique urban environment that experiences cold and dark conditions, which are crucial for ice fog formation.

Low visibility due to high air pollution levels and ice fog formation can be routine in certain seasons in Fairbanks. Fairbanks, along with the larger Fairbanks-North Star Borough, routinely experiences wintertime $PM_{2.5}$ levels > 50 g m^{-3} (Schmale et al., 2018). This is due to increased energy usage in the winter that relies on coal, gasoline, fuel oil, and residential burning (Bowling, 1986). A portion of the increased wintertime energy needs is supplied by the six power plants located in the 32 square mile area of the Fairbanks North Star Borough. Due to the cold winter temperatures, there is also increased residential heating, typically in the form of biomass burning of wood or fuel oil (Nicholls et al., 2010). Local emissions in Fairbanks are often trapped by cold temperatures and steep surface-based inversions (Tran and Mölders, 2011). The power plants,

automobiles, and the Chena River, which runs through downtown Fairbanks, provide sources of water vapor in the winter. Inversions with sufficient water vapor can also lead to ice fog which can reduce visibility down to 200 m (Schmitt et al., 2013).

The formation processes of ice fog are not well known. This is in part due to a limited understanding of the sources and microphysical properties of ice nucleating particles (INPs) and the magnitude of their effect on ice fog formation. A small but important number of particles may act as INPs by facilitating the formation of ice from supercooled droplets followed by freezing at temperatures > -38°C. This process is crucial for ice fog formation, although the cumulative impact of INPs is poorly understood (Kanji et al., 2017). Crystals in an ice fog have been shown to form via contact (i.e. formation of supercooled droplets due to aerosols first serving as cloud condensation nuclei (CCN) followed by freezing as temperatures decrease due to the ice-nucleating properties of the aerosols) or immersion freezing (i.e. the aerosols first serve as cloud condensation nuclei (CCN) and form supercooled droplets, then freezing as a result of the ice nucleating properties of the aerosol as temperatures decrease), as well as, to a lower degree, deposition freezing (i.e. water vapor directly freezing on an INP) (Gultepe et al., 2017; Huffman and Ohtake, 1971). Generally, aerosols such as sea spray, mineral dust, black carbon, and biologically-derived particles have been shown to serve as INPs (Hoose and Möhler, 2012; Petters et al., 2009; Conen et al., 2011; DeMott et al., 2018; Huang et al., 2021). However, pollution aerosols from combustion have been shown to be poor INPs compared to dust or biological particles (Bi et al., 2019). Only three studies from the 1960s and 1970s have analyzed sources of INPs in ice fog, making ice fog significantly understudied compared to other ice cloud types (Kumai, 1964; Kumai, 1966; Radke et al., 1976). Since these are the only studies to assess INPs within ice fog, there are major knowledge gaps in our understanding of how ice fog forms.

Here we analyze an ice fog episode that occurred in Fairbanks from 29 January to 3 February 2022. We present total and size-resolved INP concentration data throughout the course of the event, in addition to days prior to and after the ice fog. We also utilize bulk aerosol mass and number, metal composition, and single particle composition data to better understand the general aerosol

population sources. This is the first time a study has evaluated the sources and roles of INPs in ice fog formation in Fairbanks.

Chapter 2

DATA AND METHODS

2.1 ALPACA OVERVIEW

The Alaskan Layered Pollution And Chemical Analysis (ALPACA) study occurred from 17 January 2022 - 25 February 2022 with the goal of better understanding pollution under cold and dark conditions (Simpson et al., 2019; Simpson et al., 2023). Fairbanks, Alaska (64.8401° N, 147.7200° W), is a city with a population of 32,515 located within the Fairbanks-North Star Borough with a total population of 95,655 in the interior of Alaska. There were multiple field sites located throughout the Fairbanks-North Star Borough (Figure 2.1). While Fairbanks itself is not technically within the Arctic circle, it has a subarctic climate subjected to conditions similar to that of the Arctic and may be representative of conditions in Arctic communities. Measurements presented in our study were taken at the University of Alaska Community Technical College (CTC) site located in downtown Fairbanks. Instruments were housed in two laboratory trailers at CTC or were located outside near the containers. The ALPACA study also supported outdoor measurements at the University of Alaska Farm Field site and indoor measurements at a house in a residential community. Supplementary data used in our study were collected at Fort Wainwright (see Simpson et al., 2023 for more details). Gas, aerosol, and meteorological measurements were made at all these sites in order to complete the research objectives of the ALPACA project. During the ALPACA study, there was one major pollution event that coincided with an ice fog event.

2.2 MEASUREMENT TECHNIQUES

2.2.1 BULK AEROSOL MASS AND METAL CONCENTRATIONS

The HORIBA, Ltd. PX-375 continuous particle mass and elemental speciation monitor was used to measure PM_{10} mass concentrations (μg m^{-3}) and concentrations of various metals (ng m^{-3}) (Creamean et al., 2016). The PX-375 had a flow rate of 16.7 L min^{-1} through an EPA louvered

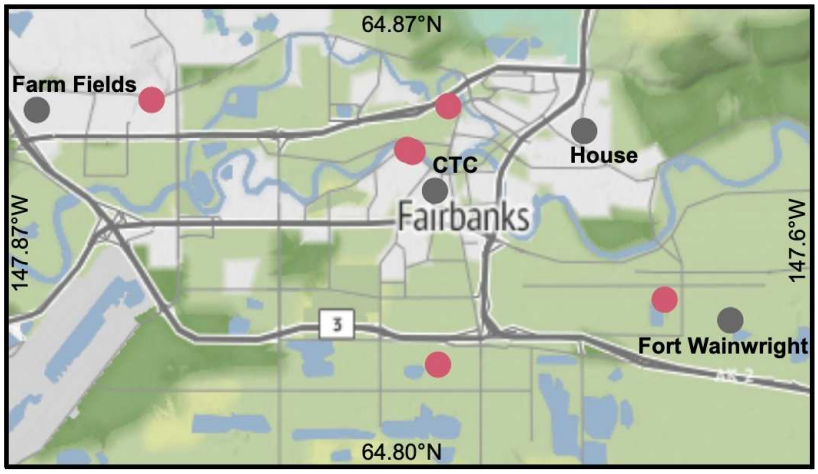

Figure 2.1: Map of Fairbanks, Alaska with study locations marked by gray points and labeled. Power plants are marked by pink points.

PM_{10} inlet. Each sample consisted of 30 minutes of ambient collection. Particles were deposited on a 100-mm diameter spot on Teflon™ PTFE fabric filter tape for beta-ray attenuation analysis for total PM_{10} mass concentrations, followed by energy dispersive x-ray fluorescence (EDXRF) analysis for concentrations of titanium, vanadium, chromium, manganese, iron, nickel, copper, zinc, arsenic, lead, aluminum, silicon, sulfur, potassium, and calcium. Lower detection limits were defined as in Creamean et al., 2016. The PX-375 was located outside of the CTC trailers within its own temperature-controlled enclosure, with the inlet located approximately 2 meters above the ground (m AGL).

2.2.2 AEROSOL NUMBER CONCENTRATIONS

Aerosols were monitored in downtown Fairbanks in one of the laboratory trailers at the CTC with a commercial optical counter (model OPC 1.109, Grimm Aerosol Technik,) at a time resolution of 1 minute. The inlet was located approximately 5 m AGL. The OPC 1.109 classifies individual particles in size within 31 channels ranging from 0.25 to 32 μm, based on the intensity of light scattered by particles illuminated by a laser diode (655 nm, Pmax = 40mW) (Heim et al., 2008; Burkart et al., 2010). As the instrument is factory-calibrated with polystyrene latex particles of controlled spherical shape and known refractive index (RI = 1.56 for PSL), and as these parameters

for complex ambient particles are not known, the size distribution measurements are expressed as optical latex equivalent diameters. Ambient air was drawn at 3.5 meters above ground level into the OPC at a volume flow rate of 1.2 L.min^{-1} through a short length ($\approx$ 1.5 m) of 1/4" o.d vertical anti-static tube extending through the shelter roof. Particle sampling efficiency was assessed using the particle loss calculator software developed by von der Weiden et al., 2009. The particle transmission was evaluated to vary between 99 and 88% for the 0.25-10 µm size range.

2.2.3 SINGLE-PARTICLE COMPOSITION

Here we include data collected by the University of Michigan. A 10-stage rotating micro-orifice uniform deposit impactor (MOUDI) was used to collect atmospheric particles onto aluminum foil substrates. It had an independent inlet out of the top of one of the CTC trailers with the top of the inlet at approximately 5 m AGL. The MOUDI sampled for 12 hours (hr) (29 January - 03 February 2022) and 24 hr (17 - 28 January 2022 and 04 - 26 February 2022) intervals corresponding with the filter sampling. Size ranges of 0.18 - 0.32 µm, 0.56 - 1.0 µm, and 1.8 - 3.2 µm were analyzed for the entire study period. Size ranges of 3.2 - 5.6 µm, 5.6 - 10 µm, and 10 - 18 µm were analyzed from 29 January - 03 February 2022. Analysis of single particles was conducted by scanning electron microscopy with energy dispersive X-ray spectroscopy (SEM-EDX) in order to determine the size, morphology, and elemental composition. Details on the analytical methods are described in Kirpes et al., 2018 and McNamara et al., 2020.

2.2.4 FILTER COLLECTION FOR TOTAL AEROSOL INP CONCENTRATIONS

Twenty-four hr (17 - 28 January 2022 and 04 - 21 February 2022) and 12 hr (29 January - 03 February 2022) integrated total aerosol samples were collected throughout ALPACA (see Table 2.1). Details on the filter unit samplers can be found in several papers, including Hill et al., 2016 and Creamean et al., 2022, but are described briefly here. This system uses a vacuum pump (Thomas oil-less piston compressor/vacuum pump) that pulls through polycarbonate filters (0.2

μm pore size backed with 10-μm polycarbonate filters) at 15 L min^{-1} on average, contained in pre-sterilized, single-use, open face Nalgene™ Sterile Analytical Filter Units. Flow rates were measured continuously in-line using a mass flow meter (TSI 5200-2). The filters were protected under a precipitation shield. The filter unit and precipitation shield were located outside 2 m AGL with tubing into a temperature-controlled enclosure to the flow meter and pump. The filters were stored frozen at -20°C from collection until analysis for 4-15 months.

2.2.5 COLLECTION OF SIZE-RESOLVED SAMPLES FOR OFFLINE INP ANALYSIS

A 4-stage Davis Rotating-drum Unit for Monitoring cascading impactor (DRUM model DA-400; DRUMAir™; Cahill et al., 1987) collected size-resolved aerosols. Similar to the MOUDI, the DRUM was located in one of the CTC trailers with a 5-m AGL independent inlet at the top of the trailer. Details on the DRUM can be found in Creamean et al., 2018, Creamean et al., 2019, and Creamean et al., 2022. Briefly, the DRUM collects aerosols via impaction on sterilized perfluoroalkoxy substrate strips coated with petrolatum at 4 size ranges from 0.15 to > 12 μm in diameter with size cuts at 2.96, 1.21, and 0.34 μm at 27 – 30 L min^{-1}. These size ranges cover many aerosols including those that serve as INPs (DeMott et al., 2010). The DRUM impactor was encased in a 47 cm × 35.7 cm × 17.6 cm Pelican™ case. During ALPACA, DRUM samples were collected at a 24 hr temporal resolution from 17 - 28 January 2022 and 04 - 25 February. DRUM samples were collected at a 12 hr temporal resolution from 29 January - 03 February 2022. The DRUM substrates were stored frozen at -20°C from collection until analysis for approximately 13-15 months. The smallest (0.15 - 0.3 μm) and largest (3-12 μm) size ranges were analyzed from 29 January 21:00 - 30 January 8:58 2022, 02 February 20:54 - 03 February 9:04 2022, 18 February 9:00 - 19 February 8:58 2022, and 24 February 9:58 - 25 February 8:51 2022. See Table A.1 for metadata for the DRUM samples. These dates were selected to quantify INP sizes during and outside of the ice fog period.

2.2.6 PROCESSING OF INP SAMPLES

Select DRUM substrates and all filter samples were processed on the Colorado State University (CSU) Ice Spectrometer (IS). Details of this process are found in Hill et al., 2016 and Creamean et al., 2022 but are described briefly here. The samples were processed by placing each substrate/filter in a 50 mL sterile polypropylene tube with 8 mL of 0.1 μm filtered deionized water and shaken at 200 rpm for 20 min to resuspend particles. The IS contains two 96-well temperature-controlled aluminum blocks fitted with disposable clean PCR (Polymerase Chain Reaction) trays. Aliquots of the aerosol suspension were dispensed into the PCR trays (under a laminar flow clean hood), the trays were placed in the metal trays in the IS, the trays covered with a plexiglass window, and headspace purged with cooled, dry N_2. Frozen aliquots of 50 μL were counted at each 0.5-degree interval as the temperature was lowered at 0.33 °C min^{-1} to –30 °C. Eight-fold dilutions were used to count INPs active at the lowest temperatures. Sample blanks were also collected and analyzed. INPs in select samples were further characterized through thermal treatments and peroxide digestions to measure the contributions of heat-labile and organic INPs, respectively (see Table 2.1). The remaining INPs are inorganic (i.e. likely mineral) in nature. To assess the fractional contribution of heat-labile, proteinaceous INPs, the sample was re-tested after heating to 95°C for 20 min (Hill et al., 2016; Suski et al., 2018; O'Sullivan et al., 2018). To remove all organic INPs, 30% H_2O_2 was added to the sample then heated to 95°C for 20 min while illuminated with UVB fluorescent bulbs to generate hydroxyl radicals (residual H_2O_2 is removed using catalase), and the samples are then again processed in the IS (Suski et al., 2018).

Table 2.1: Metadata for filter samples, including collection dates, times, and durations, and which samples were subject to INP processing, INP treatments, and levoglucosan analysis. Checkmarks indicate which filters were subject to the various analytical techniques.

Start Datetime (AKST)	End Datetime (AKST)	Collection Duration	INP Processing	INP Treatments	Levoglucosan Analysis
1/17/22 9:06	1/18/22 9:07	24 hr	✓		✓

Table 2.1 . . . continued

Start Datetime (AKST)	End Datetime (AKST)	Collection Duration	INP Processing	INP Treatments	Levoglucosan Analysis
1/18/22 9:09	1/19/22 9:32	24 hr	✓		
1/19/22 9:34	1/20/22 9:17	24 hr	✓		
1/20/22 9:22	1/21/22 9:24	24 hr	✓		
1/21/22 9:30	1/22/22 9:06	24 hr	✓		
1/22/22 9:11	1/23/22 9:02	24 hr	✓		
1/23/22 9:04	1/24/22 9:15	24 hr			
1/24/22 9:18	1/25/22 9:03	24 hr	✓		
1/25/22 9:06	1/26/22 9:16	24 hr	✓		
1/26/22 9:20	1/27/22 9:00	24 hr	✓		
1/27/22 9:06	1/28/22 8:59	24 hr	✓	✓	
1/28/22 9:03	1/29/22 9:07	24 hr	✓		
1/29/23 9:10	1/29/22 21:04	12 hr	✓		✓
1/29/22 21:07	1/30/22 9:04	12 hr	✓		
1/30/22 9:10	1/30/22 20:24	12 hr	✓		
1/30/22 20:56	1/31/22 9:18	12 hr	✓		
1/31/22 9:21	1/31/22 20:52	12 hr	✓	✓	
1/31/22 20:54	2/1/22 9:05	12 hr	✓		✓
2/1/22 9:07	2/1/22 20:58	12 hr	✓		
2/1/22 21:00	2/2/22 9:10	12 hr	✓		
2/2/22 9:11	2/2/22 20:58	12 hr	✓		
2/2/22 20:59	2/3/22 9:07	12 hr	✓	✓	
2/3/22 9:09	2/3/22 20:58	12 hr	✓		✓
2/3/22 20:59	2/4/22 9:01	12 hr	✓		✓

Table 2.1 . . . continued

Start Datetime (AKST)	End Datetime (AKST)	Collection Duration	INP Processing	INP Treatments	Levoglucosan Analysis
2/4/22 9:06	2/5/22 9:00	24 hr	✓		
2/5/22 9:03	2/6/22 9:04	24 hr	✓	✓	
2/6/22 9:07	2/7/22 9:14	24 hr	✓		
2/7/22 9:17	2/8/22 9:07	24 hr	✓		
2/8/22 9:10	2/9/22 9:08	24 hr	✓		
2/9/22 9:11	2/10/22 9:07	24 hr	✓	✓	
2/10/22 9:09	2/11/22 9:05	24 hr	✓		
2/11/22 9:09	2/12/22 9:02	24 hr	✓		
2/12/22 9:04	2/13/22 9:01	24 hr	✓		
2/13/22 9:05	2/14/22 9:06	24 hr	✓		
2/14/22 9:12	2/15/22 9:05	24 hr	✓	✓	
2/15/22 9:08	2/16/22 9:06	24 hr			
2/16/22 9:09	2/17/11 9:06	24 hr	✓		
2/17/22 9:09	2/18/22 9:03	24 hr	✓		✓
2/18/22 9:07	2/19/22 9:02	24 hr	✓		
2/19/22 9:06	2/20/22 8:57	24 hr	✓		
2/20/22 9:01	2/21/22 9:11	24 hr	✓		
2/21/22 9:15	2/22/22 9:05	24 hr	✓		

2.2.7 CONTEXTUAL METEOROLOGICAL DATA

Temperature data were collected via a thermistor epoxied onto 9-mm diameter metal tubes and placed inside PVC radiation shields (Cesler-Maloney et al., 2022). The temperature probe

used in this study was positioned 3 m AGL. The temperature sensor had a precision >0.15°C over 20 to -60°C. Wind speed and direction were measured by a wind monitor with a propeller and potentiometer. Dew point data were retrieved from Wunderground and collected at Fairbanks International Airport (FAI).

2.2.8 LEVOGLUCOSAN ANALYSIS

The levoglucosan analysis was performed with a Dionex DX-500 series ion chromatograph with pulsed amperometric detection via an ED-50/ED-50A electrochemical cell. This cell has two electrodes, a gold working electrode and a pH-Ag/AgCl (silver/silver chloride) reference electrode. Separation was employed by a sodium hydroxide gradient and a Dionex CarboPac PA-1 column (4×250mm).The run time was 59 min with an injection volume of 100µL. More details can be found in Sullivan et al., 2019 and Sullivan et al., 2022.

2.2.9 MICROPHYSICAL DATA

Data from a Particle Phase Detector–2000 (PPD2K; Vochezer et al., 2016) was used between 12:00 29 January - 9:00 3 February. The PPD2K measures the forward scattered light as particles pass through a laser beam. The scattered light can be used to measure particle shape and size. The PPD2K was operated at building 4070 at Fort Wainwright with its inlet at the ground level. More information can be found in Vas et al., 2021.

Chapter 3

RESULTS AND DISCUSSION

3.1 ICE FOG EVENT OVERVIEW

During the ALPACA study, an ice fog and pollution event occurred from 29 January to 3 February 2022 (Figure 3.1). The ice fog event was identified through the Fairbanks National Weather Service (NWS) and was further validated by microphysical data (Figure A.1). Throughout the study, temperature ranged from -30.4°C to 2.0°C and dew point ranged from -29.4 to 23.1°C. However, both were colder during the ice fog/pollution period, where temperature ranged from -20.8°C to -30.4°C and dew point ranged from -29.4°C to -16.9°C. On 31 January, the dew point was greater than temperature indicating a supersaturated environment. Outside of the pollution period, average PM_{10} was 10.6 μg/m^3 while average PM_{10} was 26.8 μg/m^3 during the pollution period, which equates to a 153% increase. Winds remained calm throughout the study period (Figure A.2).

3.2 INPS IN FAIRBANKS

Figure 3.2 displays the INP concentrations at select temperature ranges and the onset freezing temperature (i.e. the highest temperature in which drops froze and thus INPs were detected by the CSU IS) of each filter. See complete cumulative INP spectra in Figure A.3. During the ice fog period, there was a 6% decrease in INPs at -25°C and a 58% decrease in INPs at -15°C. These temperatures were chosen because there were very few INPs detected at -12.5°C and above. The lower INP concentrations during the ice fog period suggest that a subset of the INPs had already been activated into fog ice crystals and possibly not captured by the filter unit sampler, due to the relatively large size typical of ice fog crystals, which is typically < 200 μm (Gultepe et al., 2015). Measurements taken at Fort Wainwright during our study show the mean size of ice crystals were 20-30 μm, however, lower concentrations (83% < 20 μm versus 17% > 20 μm) of ice crystals at larger sizes were still present to a lesser extent (Figure A.1). Average INP onset freezing temperatures

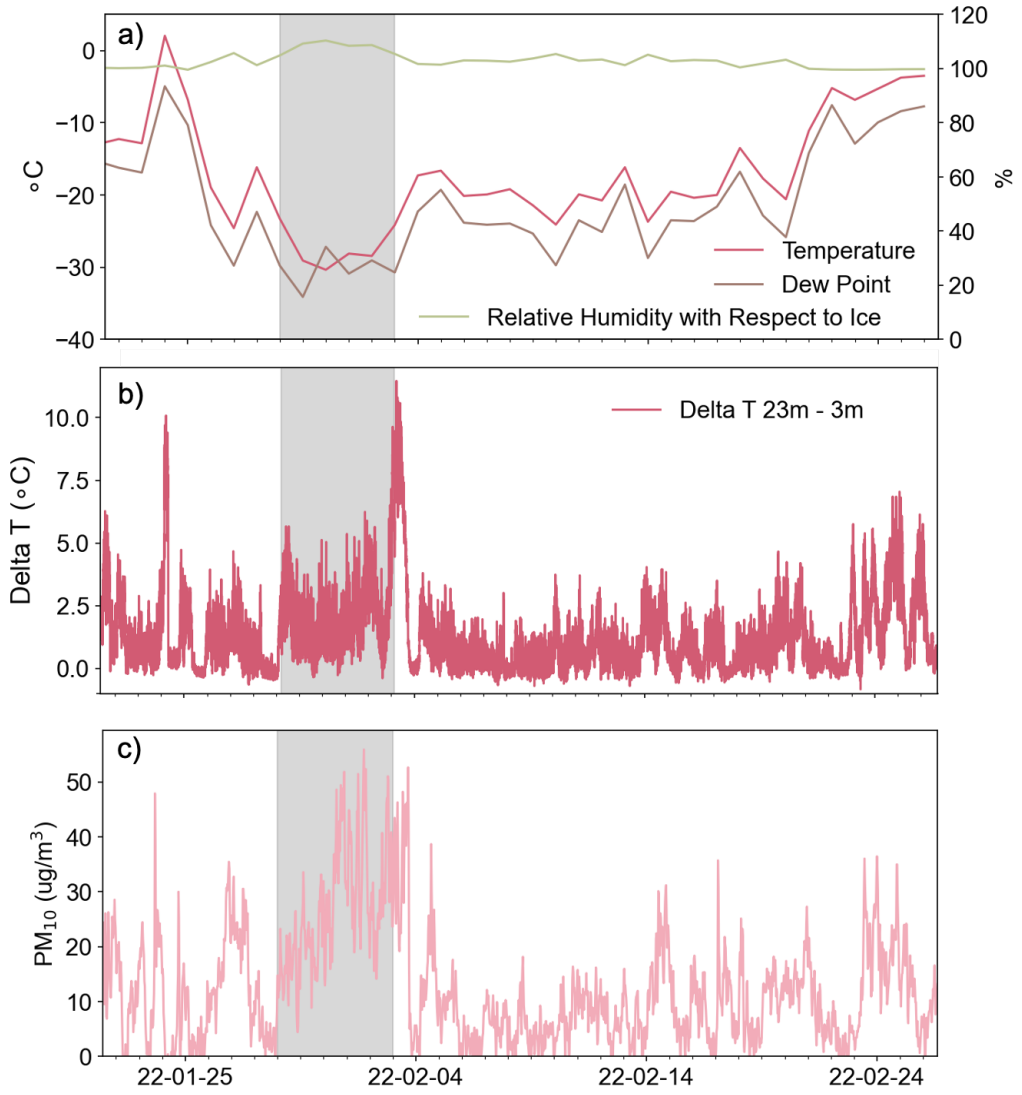

Figure 3.1: Time series of a) meteorological parameters, including air temperature, dew point, and calculated relative humidity with respect to ice (RH ice = $0.0195T^2 + 0.266T + 100.5$), b) temperature difference between 3 and 23 m (i.e., and indicator of inversion strength), and c) PM_{10} mass concentrations from the downtown Fairbanks site during the 2022 ALPACA campaign. The gray shaded regions highlight the ice fog and pollution event during the campaign.

decreased from -8°C to -11°C during the ice fog period, suggesting that a majority of INPs with higher onset temperatures had already activated into ice crystals. Within the ice fog period, we defined 3 sub periods: 1) Period 1: 29 January 9:00 - 30 January 21:00 2022, 2) Period 2: 30 January 21:00 - 1 February 21:00 2022, and 3) Period 3: 1 February 21:00 - 3 February 9:00 2022. Period 2 was the peak of the pollution event (shown in Figure 3.1 by the highest PM_{10} concentrations during ALPACA) where INPs decreased in concentration by 97% at -25°C as compared to Periods 1 and

3. Average freezing onset temperature during Period 2 decreased from -10°C to -12°C from the average of Periods 1 and 3.

To our knowledge, there are limited prior studies that have evaluated INP concentrations during ice fog events. Kikuchi, 1971a, Kikuchi, 1971b, and Kikuchi, 1972 reported measurements of CCN, INPs, and ice crystals in Antarctica and concluded that ice fog is likely the result of frozen water droplets, during a time when it was speculated that INPs were a result of meteor showers. However, there are prior studies that have evaluated ice fog residuals and have collected data needed to infer what INPs might have facilitated the formation of the ice fog crystals. Kumai, 1964 measured ice crystal residuals and showed that at -39°C, the concentration of ice fog crystals in Fairbanks was 155 crystals/cm^3, and that they were likely from oil or coal burning sources. Kumai, 1966 also measured ice fog crystal residuals in Fairbanks and reported ice fog crystal concentrations at various ice crystal diameters at -39°C. The largest concentration of ice fog crystals were observed at the following sizes: 5 μm (32 crystals/cm^3), 3 μm (28 crystals/cm^3), and 7 μm (26 crystals/cm^3), which is smaller than what was observed in our study. Kumai, 1966 also reported that the residual nuclei were both organic and inorganic particles from coal, fuel oil, and gasoline combustion.

The effectiveness of INPs from pollution is debated, with studies reporting conflicting results. Some studies show that heavy pollution has no effect on INP concentrations. For example, Chen et al., 2018 showed that there was no correlation between INP concentration and $PM_{2.5}$ or black carbon mass concentration in Beijing, China even when $PM_{2.5}$ exceeded hundreds of μg m^{-3}. Zhang et al., 2022 showed that during a dust event in Beijing, INP number concentrations increased from a background concentration of 10^1 to 10 L^1 to up to 160 L^1. They also showed that increases in black carbon did not have an effect on INP number concentrations. Borys, 1989 showed that Arctic haze aerosols have 10-1000 times lower ice nucleation rates than unpolluted Arctic air. In contrast, some studies show that pollution aerosols can serve as effective INPs. For example, Zhao et al., 2019 used 11-year continuous satellite observations from multiple satellites and cloud-resolving model simulations in East Asia and determined that polluted continental aerosols, excluding smoke and dust aerosols, contained a large fraction of INPs. Another study at the Jungfraujoch research station,

located in the Swiss Alps, found that polluted air masses from the Po Valley and industrial regions of France had increased INP concentrations > 100 L^1 relative to background conditions of 1-10 L^1 at T = 242 ± 0.4 K (Lacher et al., 2018). INP concentrations under polluted conditions from Lacher et al., 2018 are similar to the values found in our study. Schrod et al., 2020 found a moderate but significant correlation in PM_{10} and INP concentrations throughout the temperature spectrum at the Taunus Observatory (located 20 km NW of Frankfurt, Germany). Results from our study align with those demonstrating that locations subject to anthropogenic pollution can have high concentrations of INPs. These studies (and ours) might include a mixture of urban and natural sources of aerosol (i.e. they are not densely-populated urban areas like Beijing).

Compared to other Arctic and sub-Arctic continental locations where observations have been collected, Fairbanks had much higher concentrations of INPs during ALPACA. For example, Wex et al., 2019 reported on INP concentrations in multiple Arctic land-based locations and found INP concentrations between 10^{-3} - 10^{-2} L^{-1} at -20°C in Alert (Nunavut), Utqiaġvik (Alaska), Ny-Ålesund (Svalbard), and Villum Research Station (Greenland). These values are 1-3 orders of magnitude smaller than the INP concentrations found in Fairbanks at -20°C during ALPACA.

3.3 COMPOSITION AND SIZE OF INPS

Analysis of the 3 - 12 μm and 150 - 340 nm size bins of the DRUM impactor show there is at least a two order of magnitude increase in INP concentrations from 150 - 340 nm to 3-12 μm (Figure 3.3). Figure A.4 shows the complete cumulative INP spectra for these samples. In the 3-12 μm size bin, there is no apparent relationship between INP concentrations inside and outside of the ice fog period. In the 150 - 340 nm size bin, there is a 90% decrease in cumulative INPs when inside the ice fog period at -25°C, a 92% decrease in cumulative INPs at -22.5°C and a 93% decrease in cumulative INPs at -20°C. (Note the log scale in Figure 3.3.) This could indicate that relatively small INPs were selectively activated into the fog while larger INPs were always present. During the autumn and spring of the 2019-2020 Multidisciplinary drifting Observatory for the Study of Arctic Climate (MOSAiC) super-micron INPs were more abundant, except during the

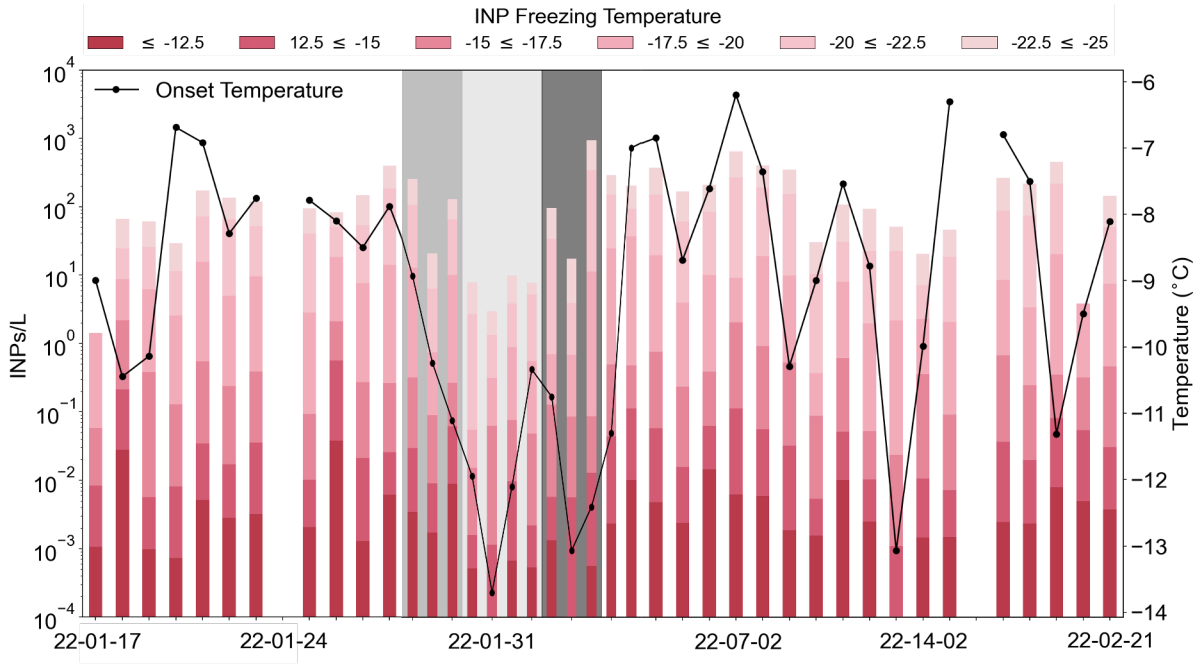

Figure 3.2: Cumulative INP concentrations per L of air at a representative set of freezing temperature values for each total aerosol filter sample collected in downtown Fairbanks at the CTC site. The ice fog period is shaded gray. The wider bars, collected between 17 - 28 January and 4 - 21 February represent the filters collected for a total of 24 hours. The narrow bars, collected between 29 January - 3 February, represent filters collected for a total of 12 hours. The first set of bars highlighted in gray represent Period 1: 29 January 9:00 - 30 January 21:00 2022, 2) Period 2: 30 January 21:00 - 1 February 21:00 2022, and 3) Period 3: 1 February 21:00 - 3 February 9:00 2022, respectively. The solid black line shows the onset freezing temperature for each filter.

winter arctic haze when pollution was transported long distances and was present in the central Arctic (Creamean et al., 2022). Creamean et al., 2018 and Creamean et al., 2019 also observed more abundant super-micron INPs when the INPs were from a local source. It has also been observed that super-micron INPs are more effective than sub-micron, when the INPs are composed of mineral dust (Reicher et al., 2019, Chen et al., 2021, Mason et al., 2016). Despite many of the INPs being organic during this study, there was still an inorganic fraction that could have potentially contributed to the large super-micron INP population (e.g. mineral dust). The possible sources of the INPs are discussed in more detail in the following sections that report on total aerosol chemical composition.

Figure 3.4 displays selected INP spectra including total INPs, INPs remaining after heat treatment (non-heat labile), and INPs remaining after peroxide treatment (inorganic, often mineral dust). During the ice fog period, peroxide treatments resulted in reductions in INPs from 20 - 99% (total

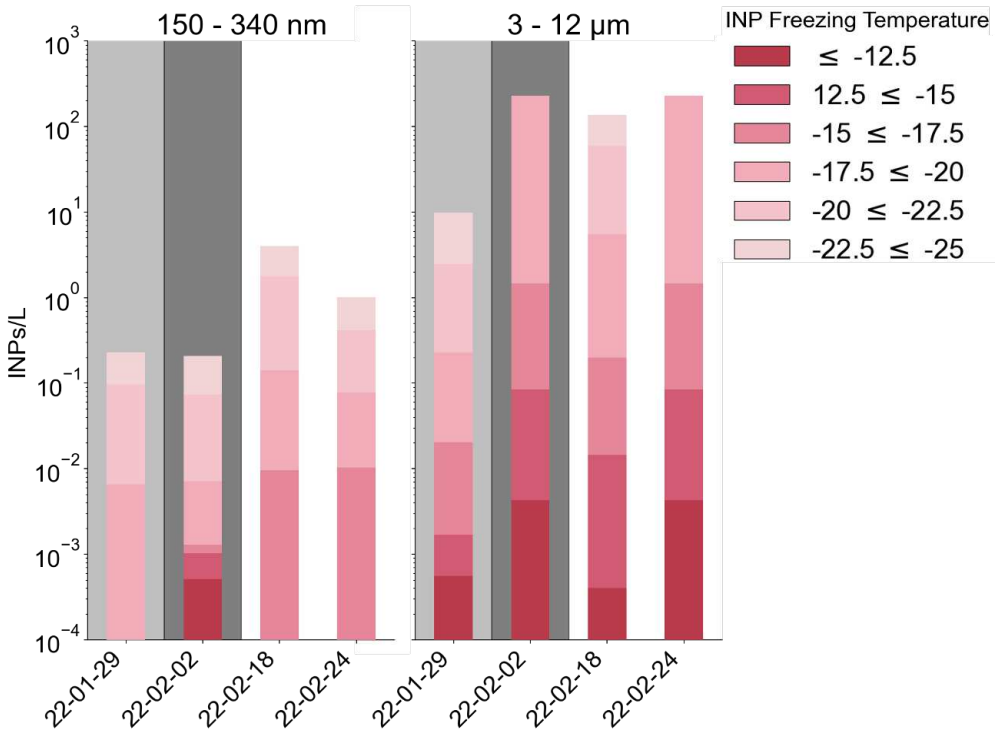

Figure 3.3: Cumulative INP concentrations at selected temperatures for 3 - 12 µm and 150 - 340 nm size bins. Gray bars indicate samples from within the ice fog period.

INP mean: 112.6 INPs/L, peroxide reduction mean: 0.4 INPs/L) at -22.5°C (the coldest temperature observed in all three spectra). Outside of the ice fog period, peroxide treatments produced (or resulted in) reductions in INPs from 98 - 99% (total INP mean: 54.6 INPs/L, peroxide reduction mean: 0.4 INPs/L) at -22.5°C. The 20% reduction in INPs occurred from 31 January 9:21 - 20:58 AKST during the peak of the fog and pollution period. The fractional contributions of INP types changed throughout ALPACA. During the non-ice fog periods, most INPs were heat-labile, followed by organic, with very few INPs being inorganic. Inorganic INPs peaked during period 2 (peak of ice fog/pollution event) while heat-labile INPs were at a low. Organic INPs peaked during periods 1 and 3.

One scenario consistent with the results of the peroxide treatments is that more efficient INPs derived from biological materials or organics that typically activate at warmer freezing temperatures (Testa et al., 2021) may have been depleted. This is consistent with the idea that biological INPs are/were activated into the fog before colder temperature INPs such as mineral dust (Koehler et al.,

2010). A dominance of organic INPs has been observed in other northern high latitude locations. Barry et al., 2023 and Creamean et al., 2020 observed that a majority of INPs in permafrost samples contained INPs that were organic. INPs from biomass burning have been shown to contain large fractions of organic INPs (Schill et al., 2020). When biomass burning aerosols dominate the aerosol distribution, organic INPs can be a significant fraction of the total INPs (Barry et al., 2021).

During the ice fog period, heat treatments produced reductions in INPs by 54 - 85% (total INP mean: 112.6 L^{-1}, heat reduction mean: 17.1 L^{-1}) at -22.5°C. Outside of the ice fog period, heat treatments reduced INPs by 54 - 97% (total INP mean: 54.6 L^{-1}, heat reduction mean: 5.6 L^{-1}) at -22.5°C. These reductions within and outside the fog period are much more similar to each other than the reductions produced from the peroxide treatments. A potential reason for this could be that the source of the biological INPs remained constant both inside and outside the fog period. Such a large biological portion of INPs in Fairbanks during the winter is unexpected due to the extremely cold temperatures and lack of vegetative/soil surfaces exposed, but our results from the ALPACA period are consistent with observations in the spring collected over the Prudhoe Bay despite most surfaces being frozen (Creamean et al., 2018). It is also important to note that certain dust types (e.g., quartz dusts, calcite) are sensitive to wet heating unlike common felsic/illitic INPs (Daily et al., 2022). This means there is a possibility that minerals may have reacted to heat treatments, although quartz dusts are minor contributors in most regions. Despite many of the INPs observed in this study being heat labile or organic, there is still a large fraction of INPs remaining during the ice fog period after the treatments that are inorganic, likely indicating the presence of dust.

3.4 TOTAL AEROSOL SIZE AND COMPOSITION

Figure 3.5 shows aerosol number concentrations for both sub-micron and super-micron aerosols throughout the duration of ALPACA. The concentration of super-micron aerosols remained fairly constant through all periods. On the other hand, submicron aerosols were slightly enhanced ($\sim$110000 #/L) in concentration and less variable towards the peak of the ice fog event in period 2. This is opposite of what was observed in the sub-micron INPs during the ice fog period as they

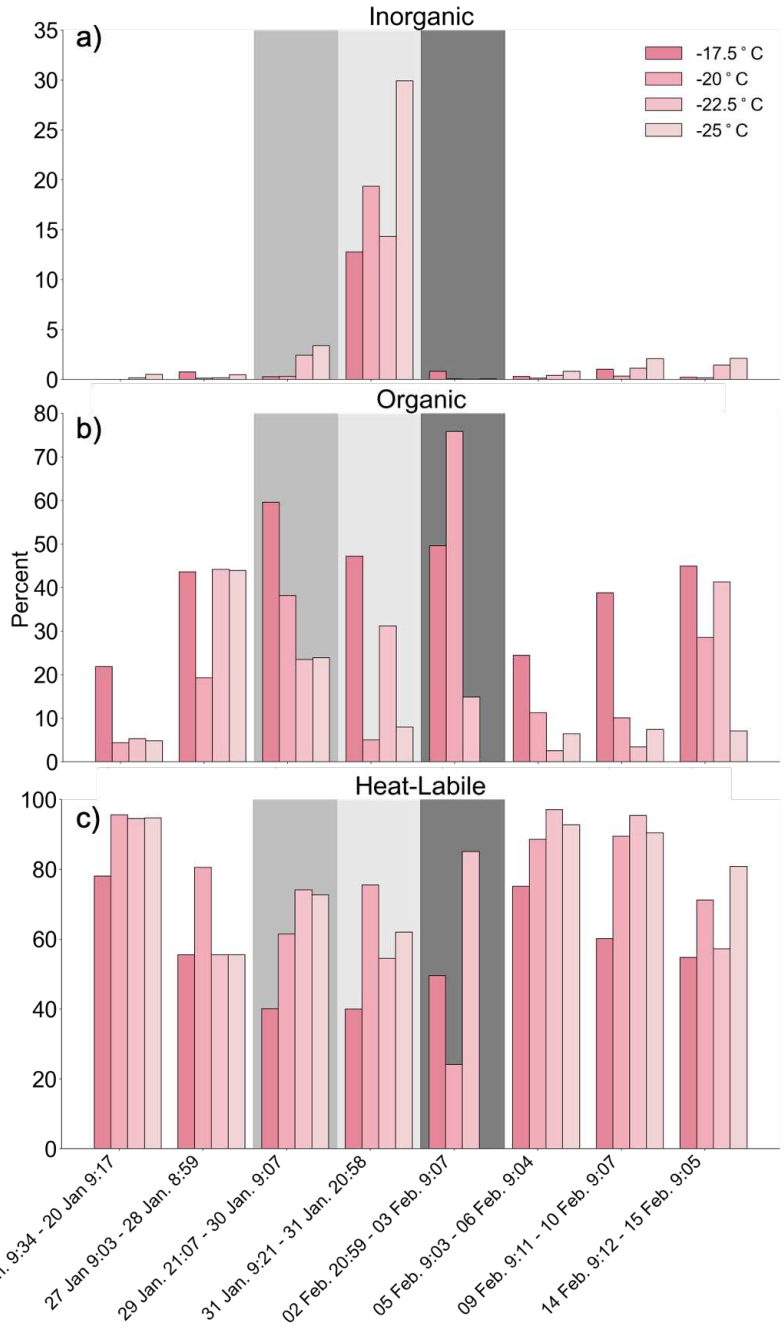

Figure 3.4: a) Percent of inorganic INPs at selected dates and temperatures, b) percent of organic INPs at selected dates and temperatures, and c) percent of heat-labile INPs for selected dates and temperatures

appeared to be depleted. This means that there were more sub-micron aerosols available to act as an INP. On the other hand, both the total aerosol and INPs did not change in the super-micron, indicating that super-micron aerosols are always present but did not affect ice fog formation to the extent of the sub-micron aerosols.

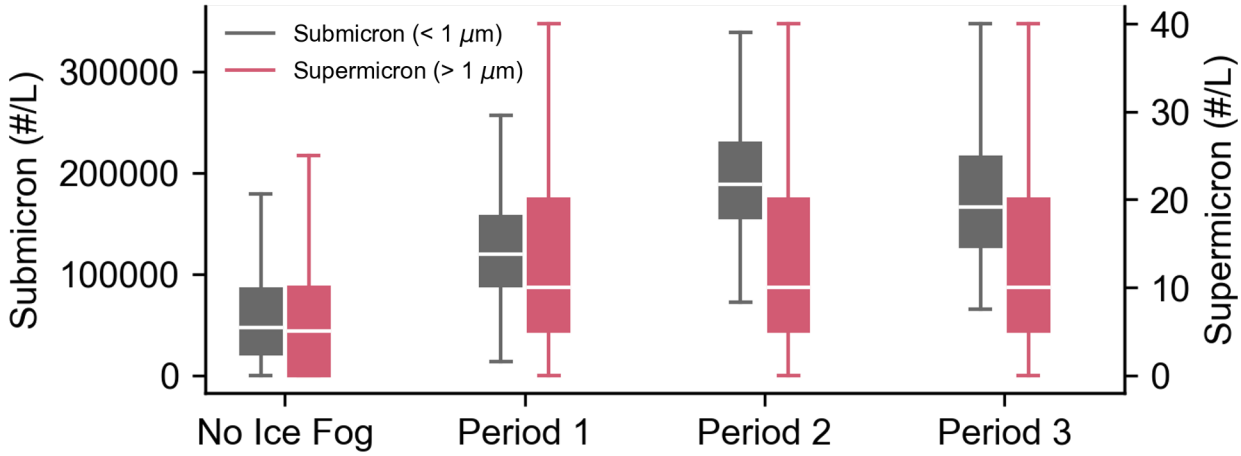

Figure 3.5: Boxplots of the total /L of sub-micron and super-micron aerosols for each of the three ice fog subperiods and the non-fog periods.

Figure 3.6 shows the fractional single particle composition of aerosols of various sizes. Throughout the size bins, dust and organic+biological aerosols dominated the aerosol population. The largest organic+biological fraction was observed in stage 1 (10-18 μm), showing that organic+biological aerosols were more frequently seen in larger size bins. The largest dust fraction was seen in stage 3 (3.2-5.6 μm), demonstrating that dust aerosols were more frequently smaller in size than organic+biological aerosols. However, this picture is complicated by the fact that ice crystals were also likely sampled with the MOUDI. Figure S5 shows the number fraction of particles below expected area diameter on different MOUDI stages during the ice fog subperiods. Particles were more frequently mis-sized on the larger MOUDI stages, but also were mis-sized up to 70% on the smaller stages (see figure A.5). This may be because ice crystals were sampled into the MOUDI, which then sublimated and left ice fog particle residuals behind. Thus, these stages are likely a mixture of interstitial aerosol that did not activate into ice and ice fog crystal residuals.

A strong correlation between levoglucosan and PM_{10} as well as the very high levoglucosan concentrations indicates that there was a strong residential wood burning influence on the aerosol population. Figure S6 shows a correlation of levoglucosan and PM_{10} (R^2 = 0.99, n = 6). Levoglucosan is a commonly used smoke marker because it is an anhydrosugar produced from the combustion of cellulose (Simoneit et al., 1999). The source of levoglucosan in Fairbanks was likely

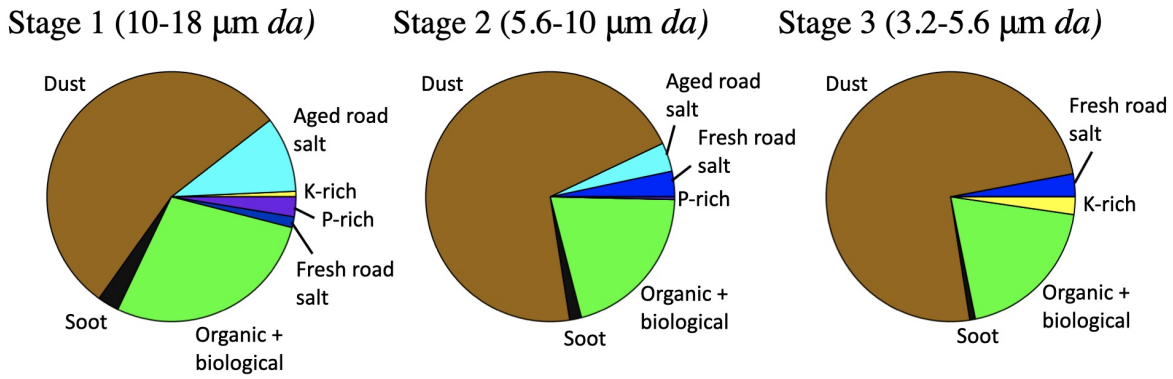

Figure 3.6: Example fractional single-particle composition on three different MOUDI stages during the ice fog.

residential wood burning. Haque et al., 2021 measured levoglucosan on the top of the International Arctic Research Center (IARC) building at UAF from June 2008 - June 2009 and found a wintertime maximum of 145 ± 47 ng m^3. Our maximum observed concentration of levoglucosan is 1190 ng m^3. This order of magnitude difference may be due to the difference in location within the city of Fairbanks (elevation = 135 m) as opposed to the top of a building located outside of downtown Fairbanks on a hill (elevation = 187 m) that might be above the buildup from local residential sources.

Finally, we used empirical orthogonal function (EOF) analysis to understand variability in PM_{10} metal composition (see Figure A.7). The analysis produced one EOF that explained over 80% of the variance in the data, and its principal component peaked during ice fog periods 2 and 3. It was composed of sulfur with some potassium, calcium, iron, and zinc, likely indicative of dust with sulfate. A dust signature peaking during the ice fog period is consistent with our filter treatment results as the percentage of inorganic INPs is highest during the ice fog period. Our EOF analysis is also consistent with the large dust fraction in the single particle composition analysis.

3.5 POTENTIAL SOURCES OF INPS IN FAIRBANKS DURING ALPACA

Based on the composition of the general aerosol population, as well as the composition of the INPs, we are able to infer there are multiple sources of INPs in Fairbanks. Due to the strong correlation between levoglucosan and PM_{10}, there is a strong wood burning influence on the general aerosol population. INP treatment data shows that there is a fairly constant and substantial presence of organic INPs. Also, organic+biological particles were the second highest relatively abundant single particle aerosol from the microscopy results. The combination of high levoglucosan concentrations, the presence of organic INPs, and organics in the single particle data indicate that residential wood burning in Fairbanks is a potential source of INPs. The high percentage of dust particles throughout the size bins in the single particle composition data paired with the increase in inorganic INPs during the ice fog period, and the EOF containing a dust signature indicate that there is additionally a dust source in Fairbanks during ALPACA. Lastly, the presence of biological particles in the single particle data as well as the high percentage of heat-labile INPs throughout our study indicate that there are highly effective biological INPs present. Altogether, we speculate the sources of aerosols, particularly that serve as INPs, are from a mixture of road dust (i.e., from gravel laid on the icy roads to increase traction) and residential wood burning. The source of the biological INPs is more challenging to pinpoint and would require further investigation.

Chapter 4

CONCLUSIONS AND FUTURE WORK

4.1 CONCLUSIONS

Here we report on INP concentrations, size, and composition, as well as single-particle composition and size during and outside of an ice fog event in Fairbanks, Alaska. Potential sources of INPs during our study are summarized in Figure 4.1. These measurements were a part of the winter 2021 ALPACA campaign with an overarching goal of better understanding atmospheric chemistry under cold and dark conditions.

We observed an ice fog event that occurred from 29 January to 3 February 2022. The ice fog was accompanied by elevated air pollution and low air temperatures. Within the ice fog event, INP concentrations decreased by 6% at -25°C and by 58% at -15°C, indicating that many INPs had already activated into ice fog crystals, especially INPs active at warmer temperatures, and were not captured by the filter units. Peroxide treatments of samples collected during the ice fog period reduced INP concentrations by 20 - 99% at -22.5°C. Outside of the ice fog period, peroxide treatments of samples reduced INPs by 98-99% at -22.5°C. Heat treatments within the ice fog period reduced INP concentrations by 54 - 85% at -22.5°C. Outside of the ice fog period, heat treatments reduced INP concentrations by 54 - 97% at -22.5°C. Together these results indicate that there was a larger inorganic fraction of INPs inside the ice fog period than outside of the ice fog period that were potentially not activated into the ice fog. The fraction of heat-labile INPs remained fairly constant both inside and outside of the ice fog period. Organic and heat-labile INPs dominated the fractional contribution of total INPs which is consistent with other northern high-latitude locations.

Analysis of INPs from the DRUM impactor showed no apparent relationship between INP concentrations inside and outside of the ice fog period in the 3 - 12 μm size bin. There was a 90% decrease in INPs in the 150 - 340 nm size bin inside the ice fog period at -25°C, a 92% decrease at -22.5°C and a 93% decrease at -20°C. This could indicate that relatively small INPs were activated

into the fog, especially considering total super-micron aerosol numbers increased during the ice fog event, meaning there was not a shortage of sub-micron aerosols to serve as INPs.

SEM-EDX data show that the general aerosol population was largely dust and organic+biological. The organic+biological aerosols were most prevalent in larger size bins, which more frequently had mis-sized particles that were likely ice fog crystals. This aligns with INP treatment results indicating that most INPs were organic and biological.

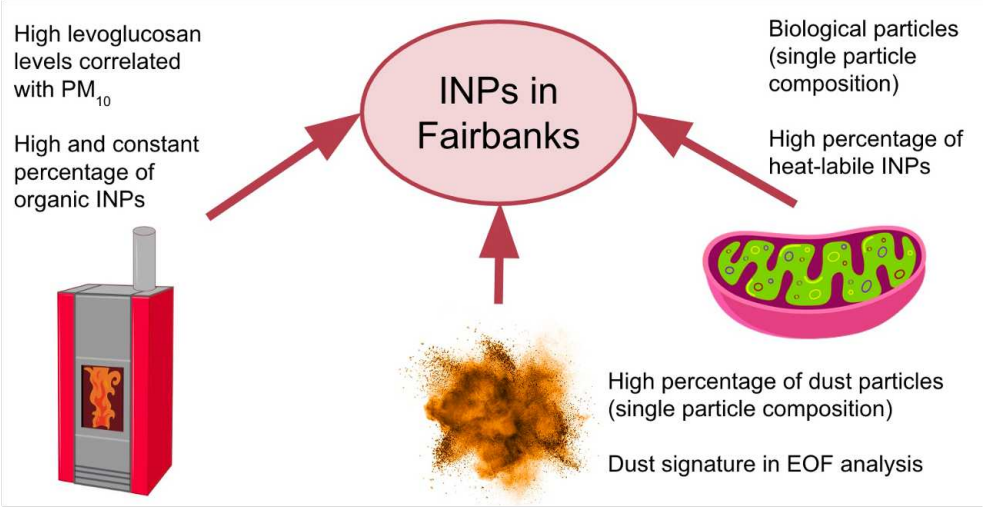

Figure 4.1: Schematic showing potential INP sources. From left to right these include: residential wood burning, dust, and biological particles.

4.2 FUTURE WORK

The analysis here is limited to a singular ice fog event in Fairbanks, Alaska. During this event, we find that most INPs that were likely activated into the ice fog crystals were organic or heat-labile, but the overall fraction of inorganic INPs increased. We also saw indications of small INPs (150 - 340 nm), as opposed to large INPs (3 - 12 μm), being activated into the fog due to a 90 - 93% decrease in concentration compared to outside of the ice fog period. In order to draw more robust conclusions about INPs in an ice fog outside of this one event, we provide the following four suggestions for future work.

1. *Comparison of INPs between ice fog events* - Work should be done utilizing the above methods and instrumentation to study how/if INPs differ between ice fog events. As there was only one ice fog event during our study, we were unable to compare INP concentration, size, and composition between different ice fog events. The general aerosol population should also be compared between events in order to understand if there is a relationship between the aerosol population and INPs between ice fog events. Ice fog events in Fairbanks typically occur from late October to mid-March and have been decreasing in frequency by 60-70% since 1948 (Hartl et al., 2023). Because of this, a field campaign focused on studying INPs in ice fog should encompass the entire late October to mid-March time frame in order to have the best chance of capturing multiple ice fog events. A field campaign encompassing this large time frame would need rotating personnel or would need to be conducted by a group who permanently resided in an area subject to ice fog.

2. *Size-resolved INP composition* - Treatments should be applied to the different DRUM stages in order to understand how INP composition differs between size bins. With these data we could better understand potential sources of INPs by knowing both their size and composition. Work could be done to compare total INP composition to size-resolved INP composition in order to determine if composition is consistent throughout different size bins. These treatments should be applied after the remaining DRUM samples are analyzed for total INPs in order to fill in temporal gaps.

3. *Online INP data* - INP concentration data from a Continuous Flow Diffusion Chamber (DeMott et al., 2015; Bi et al., 2019) collected during the campaign offers an opportunity to learn about how INPs vary in real time. The filter data collected in this study allow us to understand how INPs vary between 12 - 24 hr periods. However, the CFDC data would allow us to understand how INPs vary with these larger time frames and allow us to better correlate them with potential sources. Unfortunately, CFDC data were not available during the ice fog period in our study so it would be beneficial to utilize a CFDC alongside filters during another field campaign.

4. *INPs from other locations with ice fog* - INPs should be studied within ice fog in a location other than Fairbanks. Intercomparison work should be done in order to determine if the concentration, composition, and size of INPs in ice fog are dependent on location. As Fairbanks is a unique sub-Arctic city due to its high levels of pollution and strong inversion, we would expect to see a different composition of INPs.

REFERENCES

Kathy S. Law and Andreas Stohl. Arctic air pollution: origins and impacts. *Science (New York, N.Y.)*, 315(5818):1537–1540, March 2007. ISSN 1095-9203. doi: 10.1126/science.1137695.

Katharine S. Law, Andreas Stohl, Patricia K. Quinn, Charles A. Brock, John F. Burkhart, Jean-Daniel Paris, Gerard Ancellet, Hanwant B. Singh, Anke Roiger, Hans Schlager, Jack Dibb, Daniel J. Jacob, Steve R. Arnold, Jacques Pelon, and Jennie L. Thomas. Arctic Air Pollution: New Insights from POLARCAT-IPY. *Bulletin of the American Meteorological Society*, 95(12): 1873–1895, December 2014. ISSN 0003-0007, 1520-0477. doi: 10.1175/BAMS-D-13-00017.1. URL https://journals.ametsoc.org/view/journals/bams/95/12/bams-d-13-00017.1.xml. Publisher: American Meteorological Society Section: Bulletin of the American Meteorological Society.

I. J. Simpson, S. K. Akagi, B. Barletta, N. J. Blake, Y. Choi, G. S. Diskin, A. Fried, H. E. Fuelberg, S. Meinardi, F. S. Rowland, S. A. Vay, A. J. Weinheimer, P. O. Wennberg, P. Wiebring, A. Wisthaler, M. Yang, R. J. Yokelson, and D. R. Blake. Boreal forest fire emissions in fresh Canadian smoke plumes: C_1-C_{10} volatile organic compounds (VOCs), CO_2, CO, NO_2, NO, HCN and CH_3CN. *Atmospheric Chemistry and Physics*, 11(13):6445–6463, July 2011. ISSN 1680-7316. doi: 10.5194/acp-11-6445-2011. URL https://acp.copernicus.org/articles/11/6445/2011/. Publisher: Copernicus GmbH.

Seung Hyun Lucia Woo, Jia Coco Liu, Xu Yue, Loretta J. Mickley, and Michelle L. Bell. Air pollution from wildfires and human health vulnerability in Alaskan communities under climate change. *Environmental Research Letters*, 15(9):094019, August 2020. ISSN 1748-9326. doi: 10.1088/1748-9326/ab9270. URL https://dx.doi.org/10.1088/1748-9326/ab9270. Publisher: IOP Publishing.

J. Schmale, S. R. Arnold, K. S. Law, T. Thorp, S. Anenberg, W. R. Simpson, J. Mao, and K. A. Pratt. Local Arctic Air Pollution: A Neglected but Serious Problem. *Earth's Future*, 6(10): 1385–1412, 2018. ISSN 2328-4277. doi: 10.1029/2018EF000952. URL https://onlinelibrary.wiley.com/doi/abs/10.1029/2018EF000952. _eprint: https://onlinelibrary.wiley.com/doi/pdf/10.1029/2018EF000952.

Gail Fondahl and Joan Nymand Larsen. The Arctic Human Development Report II: A Contribution to Arctic Policy Shaping. In *Arctic Yearbook 2015*. 2015.

Magnus Kramshøj, Ida Vedel-Petersen, Michelle Schollert, Åsmund Rinnan, Josephine Nymand, Helge Ro-Poulsen, and Riikka Rinnan. Large increases in Arctic biogenic volatile emissions are a direct effect of warming. *Nature Geoscience*, 9(5):349–352, May 2016. ISSN 1752-0908. doi: 10.1038/ngeo2692. URL https://www.nature.com/articles/ngeo2692. Number: 5 Publisher: Nature Publishing Group.

Can Li, N. Christina Hsu, Andrew M. Sayer, Nickolay A. Krotkov, Joshua S. Fu, Lok N. Lamsal, Jaehwa Lee, and Si-Chee Tsay. Satellite observation of pollutant emissions from gas flaring

activities near the Arctic. *Atmospheric Environment*, 133:1–11, May 2016. ISSN 1352-2310. doi: 10.1016/j.atmosenv.2016.03.019. URL https://www.sciencedirect.com/science/article/pii/S1352231016301893.

Kathy S. Law, Anke Roiger, Jennie L. Thomas, Louis Marelle, Jean-Christophe Raut, Stig Dalsøren, Jan Fuglestvedt, Paolo Tuccella, Bernadett Weinzierl, and Hans Schlager. Local Arctic air pollution: Sources and impacts. *Ambio*, 46(3):453–463, December 2017. ISSN 1654-7209. doi: 10.1007/s13280-017-0962-2. URL https://doi.org/10.1007/s13280-017-0962-2.

P. L. Joyce, R. von Glasow, and W. R. Simpson. The fate of NO_x emissions due to nocturnal oxidation at high latitudes: 1-D simulations and sensitivity experiments. *Atmospheric Chemistry and Physics*, 14(14):7601–7616, July 2014. ISSN 1680-7316. doi: 10.5194/acp-14-7601-2014. URL https://acp.copernicus.org/articles/14/7601/2014/. Publisher: Copernicus GmbH.

Gerd Wendler and K. O. L. F. Jayaweera. Some measurements of the development of the surface inversion in Central Alaska during winter. *pure and applied geophysics*, 99(1):209–221, December 1972. ISSN 1420-9136. doi: 10.1007/BF00875277. URL https://doi.org/10.1007/BF00875277.

Huy N. Q. Tran and Nicole Mölders. Investigations on meteorological conditions for elevated PM2.5 in Fairbanks, Alaska. *Atmospheric Research*, 99(1):39–49, January 2011. ISSN 0169-8095. doi: 10.1016/j.atmosres.2010.08.028. URL https://www.sciencedirect.com/science/article/pii/S0169809510002371.

Meeta Cesler-Maloney, William R. Simpson, Tate Miles, Jingqiu Mao, Kathy S. Law, and Tjarda J. Roberts. Differences in Ozone and Particulate Matter Between Ground Level and 20 m Aloft are Frequent During Wintertime Surface-Based Temperature Inversions in Fairbanks, Alaska. *Journal of Geophysical Research: Atmospheres*, 127(10):e2021JD036215, 2022. ISSN 2169-8996. doi: 10.1029/2021JD036215. URL https://onlinelibrary.wiley.com/doi/abs/10.1029/2021JD036215. _eprint: https://onlinelibrary.wiley.com/doi/pdf/10.1029/2021JD036215.

Ronald A. Willis and Gary K. Grice. The Wintertime Arctic Front and Its Effect on Fairbanks, Alaska. *Monthly Weather Review*, 105(1):78–85, January 1977. ISSN 1520-0493, 0027-0644. doi: 10.1175/1520-0493(1977)105<0078:TWAFAI>2.0.CO;2. URL https://journals.ametsoc.org/view/journals/mwre/105/1/1520-0493_1977_105_0078_twafai_2_0_co_2.xml. Publisher: American Meteorological Society Section: Monthly Weather Review.

Ismail Gultepe, Andrew Heymsfield, Martin Gallagher, Luisa Ickes, and Darrel Baumgardner. Ice Fog: The Current State of Knowledge and Future Challenges. *American Meteorological Society : Meteorological Monographs*, pages 4.3–4.24, October 2017. doi: 10.1175/AMSMONOGRAPHS-D-17-0002.1. URL https://journals.ametsoc.org/view/journals/amsm/58/1/amsmonographs-d-17-0002.1.xml.

I. Gultepe, T. Kuhn, M. Pavolonis, C. Calvert, J. Gurka, A. J. Heymsfield, P. S. K. Liu, B. Zhou, R. Ware, B. Ferrier, J. Milbrandt, and B. Bernstein. Ice Fog in Arctic During FRAM–Ice Fog Project: Aviation and Nowcasting Applications. *Bulletin of the American Meteorological Society*, 95(2):211–226, February 2014. ISSN 0003-0007, 1520-0477. doi:

10.1175/BAMS-D-11-00071.1. URL https://journals.ametsoc.org/view/journals/bams/95/2/bams-d-11-00071.1.xml. Publisher: American Meteorological Society Section: Bulletin of the American Meteorological Society.

Elmer Robinson, William C. Thuman, and Ernest J. Wiggins. Ice Fog as a Problem of Air Pollution in the Arctic. *ARCTIC*, pages 88–104, January 1957. ISSN 1923-1245. doi: 10.14430/arctic3756. URL https://journalhosting.ucalgary.ca/index.php/arctic/article/view/66806.

Sue Ann Bowling. Climatology of High-Latitude Air Pollution as Illustrated by Fairbanks and Anchorage, Alaska. *Journal of Climate and Applied Meteorology*, 25(1):22–34, 1986. ISSN 0733-3021. URL https://www.jstor.org/stable/26182456. Publisher: American Meteorological Society.

David L. Nicholls, Allen M. Brackley, and Valerie Barber. Wood energy for residential heating in Alaska: current conditions, attitudes, and expected use. *Gen. Tech. Rep. PNW-GTR-826. Portland, OR: U.S. Department of Agriculture, Forest Service, Pacific Northwest Research Station. 30 p. 2010*, 826, 2010. doi: 10.2737/PNW-GTR-826. URL https://www.fs.usda.gov/research/treesearch/35579.

Carl G. Schmitt, Martin Stuefer, Andrew J. Heymsfield, and Chang Ki Kim. The microphysical properties of ice fog measured in urban environments of Interior Alaska. *Journal of Geophysical Research: Atmospheres*, 118(19):11,136–11,147, 2013. ISSN 2169-8996. doi: 10.1002/jgrd.50822. URL https://onlinelibrary.wiley.com/doi/abs/10.1002/jgrd.50822. _eprint: https://onlinelibrary.wiley.com/doi/pdf/10.1002/jgrd.50822.

Zamin A. Kanji, Luis A. Ladino, Heike Wex, Yvonne Boose, Monika Burkert-Kohn, Daniel J. Cziczo, and Martina Krämer. Overview of Ice Nucleating Particles. *Meteorological Monographs*, 58(1):1.1–1.33, January 2017. doi: 10.1175/AMSMONOGRAPHS-D-16-0006.1. URL https://journals.ametsoc.org/view/journals/amsm/58/1/amsmonographs-d-16-0006.1.xml. Publisher: American Meteorological Society Section: Meteorological Monographs.

P. J. Huffman and T. Ohtake. Formation and growth of ice fog particles at Fairbanks, Alaska. *Journal of Geophysical Research (1896-1977)*, 76(3):657–665, 1971. ISSN 2156-2202. doi: 10.1029/JC076i003p00657. URL https://onlinelibrary.wiley.com/doi/abs/10.1029/JC076i003p00657. _eprint: https://onlinelibrary.wiley.com/doi/pdf/10.1029/JC076i003p00657.

C. Hoose and O. Möhler. Heterogeneous ice nucleation on atmospheric aerosols: a review of results from laboratory experiments. *Atmospheric Chemistry and Physics*, 12(20):9817–9854, October 2012. ISSN 1680-7316. doi: 10.5194/acp-12-9817-2012. URL https://acp.copernicus.org/articles/12/9817/2012/acp-12-9817-2012.html. Publisher: Copernicus GmbH.

Markus D. Petters, Matthew T. Parsons, Anthony J. Prenni, Paul J. DeMott, Sonia M. Kreidenweis, Christian M. Carrico, Amy P. Sullivan, Gavin R. McMeeking, Ezra Levin, Cyle E. Wold, Jeffrey L. Collett Jr., and Hans Moosmüller. Ice nuclei emissions from biomass burning. *Journal of Geophysical Research: Atmospheres*, 114(D7), 2009. ISSN 2156-2202. doi:

10.1029/2008JD011532. URL https://onlinelibrary.wiley.com/doi/abs/10.1029/2008JD011532. _eprint: https://onlinelibrary.wiley.com/doi/pdf/10.1029/2008JD011532.

F. Conen, C. E. Morris, J. Leifeld, M. V. Yakutin, and C. Alewell. Biological residues define the ice nucleation properties of soil dust. *Atmospheric Chemistry and Physics*, 11(18):9643–9648, September 2011. ISSN 1680-7316. doi: 10.5194/acp-11-9643-2011. URL https://acp.copernicus.org/articles/11/9643/2011/. Publisher: Copernicus GmbH.

Paul J. DeMott, Ryan H. Mason, Christina S. McCluskey, Thomas C. J. Hill, Russell J. Perkins, Yury Desyaterik, Allan K. Bertram, Jonathan V. Trueblood, Vicki H. Grassian, Yuqing Qiu, Valeria Molinero, Yutaka Tobo, Camille M. Sultana, Christopher Lee, and Kimberly A. Prather. Ice nucleation by particles containing long-chain fatty acids of relevance to freezing by sea spray aerosols. *Environmental Science: Processes & Impacts*, 20(11):1559–1569, November 2018. ISSN 2050-7895. doi: 10.1039/C8EM00386F. URL https://pubs.rsc.org/en/content/articlelanding/2018/em/c8em00386f. Publisher: The Royal Society of Chemistry.

Shu Huang, Wei Hu, Jie Chen, Zhijun Wu, Daizhou Zhang, and Pingqing Fu. Overview of biological ice nucleating particles in the atmosphere. *Environment International*, 146:106197, January 2021. ISSN 0160-4120. doi: 10.1016/j.envint.2020.106197. URL https://www.sciencedirect.com/science/article/pii/S0160412020321528.

K. Bi, G. R. McMeeking, D. P. Ding, E. J. T. Levin, P. J. DeMott, D. L. Zhao, F. Wang, Q. Liu, P. Tian, X. C. Ma, Y. B. Chen, M. Y. Huang, H. L. Zhang, T. D. Gordon, and P. Chen. Measurements of Ice Nucleating Particles in Beijing, China. *Journal of Geophysical Research (Atmospheres)*, 124:8065–8075, July 2019. ISSN 0148-0227. doi: 10.1029/2019JD030609. URL https://ui.adsabs.harvard.edu/abs/2019JGRD..124.8065B. ADS Bibcode: 2019JGRD..124.8065B.

Motoi Kumai. A study of ice fog and ice-fog nuclei at Fairbanks, Alaska, Part I. Report, Cold Regions Research and Engineering Laboratory (U.S.), August 1964. URL https://erdc-library.erdc.dren.mil/jspui/handle/11681/5757. Accepted: 2016-03-21T21:08:17Z Publication Title: This Digital Resource was created from scans of the Print Resource.

Motoi Kumai. Electron Microscopic Study of Ice-Fog and Ice-Crystal Nuclei in Alaska. *Journal of the Meteorological Society of Japan. Ser. II*, 44(3):185–194, 1966. doi: 10.2151/jmsj1965.44.3_185.

Lawrence F. Radke, Peter V. Hobbs, and John E. Pinnons. Observations of Cloud Condensation Nuclei, Sodium-Containing Particles, Ice Nuclei and the Light-Scattering Coefficient Near Barrow, Alaska. *Journal of Applied Meteorology (1962-1982)*, 15(9):982–995, 1976. ISSN 0021-8952. URL https://www.jstor.org/stable/26177310. Publisher: American Meteorological Society.

William Simpson, Kathy Law, Julia Schmale, Kerri Pratt, Stephen Arnold, Jingqiu Mao, Becky Alexander, Susan Anenberg, Alexander Baklanov, David Bell, Steve Brown, Jessie Creamean, Gijs de Boer, Peter DeCarlo, Stefano Descari, Robert Elleman, James Flynn, Javier Fochesatto, Laurens Ganzenfeld, Ian Gilmour, Robert Griffin, Leena Järvi, Susan Kaspari, Pavel

Konstantinov, Jennifer Murphy, Tuukka Petäjä, Havala Pye, Jean-Christophe Raut, Tjarda Roberts, Manabu Shiraiwa, Jochen Stutz, Jennie Thomas, Joel Thornton, Krisina Wagstrom, Rodney Weber, Peter Webley, and Brent Williams. Alaskan Layered Pollution And Chemical Analysis (ALPACA) White Paper. 2019.

William R. Simpson, Jingqiu Mao, Gilberto Fochesatto, Kathy S. Law, Peter DeCarlo, Julia Schmale, Kerri Pratt, Steve R. Arnold, Jochen Stutz, Jack Dibb, Jessie M. Creamean, Rodney Weber, Brent Williams, Becky Alexander, Lu Hu, Robert J. Yokelson, Manabu Shiraiwa, Stefano Descari, Cort Anastasio, Barbara D'Anna, Rob Gilliam, Athanasios Nenes, Jason St. Clair, Barbara Trost, James Flynn, Joel Savarino, Laura Conner, Nathan Kettle, Krista Heeringa, Sarah Albertin, Andrea Baccarini, Brice Barret, Michael Battaglia, Slimane Bekki, T.J. Brado, Natalie Brett, David Brus, James R. Campbell, Meeta Cesler-Maloney, Conor J.S. Dennehy, Elsa Dieudonné, Kayane K. Dingilian, Antonio Donateo, Konstantinos M. Doulgeris, Kasey C. Edwards, Kathleen Fahey, Ting Fang, Fangzhou Guo, Laura M. D. Heinlein, Andrew L. Holen, Deanna Huff, Amna Ijaz, Sarah Johnson, Sukriti Kapur, Damien Ketcherside, Ezra J. T. Levin, Emily Lill, Allison Moon, Tatsuo Onishi, Gianluca Pappaccogli, Russell J. Perkins, Roman Pohorsky, Jean-Christophe Raut, Francois Ravetta, Tjarda Roberts, Ellis S. Robinson, Federico Scoto, Vanessa Selimovic, Michael O. Sunday, Brice Temime-Roussel, Xinxiu Tian, Judy Wu, and Yuhan Yang. Overview of the Alaskan Layered Pollutation and Chemical Analysis (ALPACA) field experiement. 2023.

Jessie M. Creamean, Paul J. Neiman, Timothy Coleman, Christoph J. Senff, Guillaume Kirgis, Raul J. Alvarez, and Atsushi Yamamoto. Colorado air quality impacted by long-range-transported aerosol: a set of case studies during the 2015 Pacific Northwest fires. *Atmospheric Chemistry and Physics*, 16(18):12329–12345, September 2016. ISSN 1680-7316. doi: 10.5194/acp-16-12329-2016. URL https://acp.copernicus.org/articles/16/12329/2016/. Publisher: Copernicus GmbH.

Michael Heim, Benjamin J. Mullins, Heinz Umhauer, and Gerhard Kasper. Performance evaluation of three optical particle counters with an efficient "multimodal" calibration method. *Journal of Aerosol Science*, 39(12):1019–1031, December 2008. ISSN 0021-8502. doi: 10.1016/j.jaerosci.2008.07.006. URL https://www.sciencedirect.com/science/article/pii/S0021850208001365.

J. Burkart, G. Steiner, G. Reischl, H. Moshammer, M. Neuberger, and R. Hitzenberger. Characterizing the performance of two optical particle counters (Grimm OPC1.108 and OPC1.109) under urban aerosol conditions. *Journal of Aerosol Science*, 41(10):953–962, October 2010. ISSN 0021-8502. doi: 10.1016/j.jaerosci.2010.07.007. URL https://www.ncbi.nlm.nih.gov/pmc/articles/PMC2954282/.

S.-L. von der Weiden, F. Drewnick, and S. Borrmann. Particle Loss Calculator – a new software tool for the assessment of the performance of aerosol inlet systems. *Atmospheric Measurement Techniques*, 2(2):479–494, September 2009. ISSN 1867-1381. doi: 10.5194/amt-2-479-2009. URL https://amt.copernicus.org/articles/2/479/2009/. Publisher: Copernicus GmbH.

Rachel M. Kirpes, Amy L. Bondy, Daniel Bonanno, Ryan C. Moffet, Bingbing Wang, Alexander Laskin, Andrew P. Ault, and Kerri A. Pratt. Secondary sulfate is internally mixed with sea spray

aerosol and organic aerosol in the winter Arctic. *Atmospheric Chemistry and Physics*, 18(6): 3937–3949, March 2018. ISSN 1680-7316. doi: 10.5194/acp-18-3937-2018. URL https://acp.copernicus.org/articles/18/3937/2018/. Publisher: Copernicus GmbH.

Stephen M. McNamara, Katheryn R. Kolesar, Siyuan Wang, Rachel M. Kirpes, Nathaniel W. May, Matthew J. Gunsch, Ryan D. Cook, Jose D. Fuentes, Rebecca S. Hornbrook, Eric C. Apel, Swarup China, Alexander Laskin, and Kerri A. Pratt. Observation of Road Salt Aerosol Driving Inland Wintertime Atmospheric Chlorine Chemistry. *ACS Central Science*, 6(5):684–694, May 2020. ISSN 2374-7943. doi: 10.1021/acscentsci.9b00994. URL https://doi.org/10.1021/acscentsci.9b00994. Publisher: American Chemical Society.

Tom C. J. Hill, Paul J. DeMott, Yutaka Tobo, Janine Fröhlich-Nowoisky, Bruce F. Moffett, Gary D. Franc, and Sonia M. Kreidenweis. Sources of organic ice nucleating particles in soils. *Atmospheric Chemistry and Physics*, 16(11):7195–7211, June 2016. ISSN 1680-7316. doi: 10.5194/acp-16-7195-2016. URL https://acp.copernicus.org/articles/16/7195/2016/. Publisher: Copernicus GmbH.

Jessie M. Creamean, Kevin Barry, Thomas C. J. Hill, Carson Hume, Paul J. DeMott, Matthew D. Shupe, Sandro Dahlke, Sascha Willmes, Julia Schmale, Ivo Beck, Clara J. M. Hoppe, Allison Fong, Emelia Chamberlain, Jeff Bowman, Randall Scharien, and Ola Persson. Annual cycle observations of aerosols capable of ice formation in central Arctic clouds. *Nature Communications*, 13(1):3537, June 2022. ISSN 2041-1723. doi: 10.1038/s41467-022-31182-x. URL https://www.nature.com/articles/s41467-022-31182-x. Number: 1 Publisher: Nature Publishing Group.

Thomas A. Cahill, Patrick J. Feeney, and Robert A. Eldred. Size-time composition profile of aerosols using the drum sampler. *Nuclear Instruments and Methods in Physics Research Section B: Beam Interactions with Materials and Atoms*, 22(1):344–348, March 1987. ISSN 0168-583X. doi: 10.1016/0168-583X(87)90355-7. URL https://www.sciencedirect.com/science/article/pii/0168583X87903557.

Jessie M. Creamean, Rachel M. Kirpes, Kerri A. Pratt, Nicholas J. Spada, Maximilian Maahn, Gijs de Boer, Russell C. Schnell, and Swarup China. Marine and terrestrial influences on ice nucleating particles during continuous springtime measurements in an Arctic oilfield location. *Atmospheric Chemistry and Physics*, 18(24):18023–18042, December 2018. ISSN 1680-7316. doi: 10.5194/acp-18-18023-2018. URL https://acp.copernicus.org/articles/18/18023/2018/. Publisher: Copernicus GmbH.

Jessie M. Creamean, Claudia Mignani, Nicolas Bukowiecki, and Franz Conen. Using freezing spectra characteristics to identify ice-nucleating particle populations during the winter in the Alps. *Atmospheric Chemistry and Physics*, 19(12):8123–8140, June 2019. ISSN 1680-7316. doi: 10.5194/acp-19-8123-2019. URL https://acp.copernicus.org/articles/19/8123/2019/. Publisher: Copernicus GmbH.

P. J. DeMott, A. J. Prenni, X. Liu, S. M. Kreidenweis, M. D. Petters, C. H. Twohy, M. S. Richardson, T. Eidhammer, and D. C. Rogers. Predicting global atmospheric ice nuclei distributions and their impacts on climate. *Proceedings of the National Academy of Sciences*, 107

(25):11217–11222, June 2010. doi: 10.1073/pnas.0910818107. URL https://www.pnas.org/doi/full/10.1073/pnas.0910818107. Publisher: Proceedings of the National Academy of Sciences.

Kaitlyn J. Suski, Tom C. J. Hill, Ezra J. T. Levin, Anna Miller, Paul J. DeMott, and Sonia M. Kreidenweis. Agricultural harvesting emissions of ice-nucleating particles. *Atmospheric Chemistry and Physics*, 18(18):13755–13771, September 2018. ISSN 1680-7316. doi: 10.5194/acp-18-13755-2018. URL https://acp.copernicus.org/articles/18/13755/2018/. Publisher: Copernicus GmbH.

D. O'Sullivan, M. P. Adams, M. D. Tarn, A. D. Harrison, J. Vergara-Temprado, G. C. E. Porter, M. A. Holden, A. Sanchez-Marroquin, F. Carotenuto, T. F. Whale, J. B. McQuaid, R. Walshaw, D. H. P. Hedges, I. T. Burke, Z. Cui, and B. J. Murray. Contributions of biogenic material to the atmospheric ice-nucleating particle population in North Western Europe. *Scientific Reports*, 8(1): 13821, September 2018. ISSN 2045-2322. doi: 10.1038/s41598-018-31981-7. URL https://www.nature.com/articles/s41598-018-31981-7. Number: 1 Publisher: Nature Publishing Group.

A. P. Sullivan, H. Guo, J. C. Schroder, P. Campuzano-Jost, J. L. Jimenez, T. Campos, V. Shah, L. Jaeglé, B. H. Lee, F. D. Lopez-Hilfiker, J. A. Thornton, S. S. Brown, and R. J. Weber. Biomass Burning Markers and Residential Burning in the WINTER Aircraft Campaign. *Journal of Geophysical Research: Atmospheres*, 124(3):1846–1861, 2019. ISSN 2169-8996. doi: 10.1029/2017JD028153. URL https://onlinelibrary.wiley.com/doi/abs/10.1029/2017JD028153. _eprint: https://onlinelibrary.wiley.com/doi/pdf/10.1029/2017JD028153.

Amy P. Sullivan, Rudra P. Pokhrel, Yingjie Shen, Shane M. Murphy, Darin W. Toohey, Teresa Campos, Jakob Lindaas, Emily V. Fischer, and Jeffrey L. Collett Jr. Examination of brown carbon absorption from wildfires in the western US during the WE-CAN study. *Atmospheric Chemistry and Physics*, 22(20):13389–13406, October 2022. ISSN 1680-7316. doi: 10.5194/acp-22-13389-2022. URL https://acp.copernicus.org/articles/22/13389/2022/. Publisher: Copernicus GmbH.

P. Vochezer, E. Järvinen, R. Wagner, P. Kupiszewski, T. Leisner, and M. Schnaiter. In situ characterization of mixed phase clouds using the Small Ice Detector and the Particle Phase Discriminator. *Atmospheric Measurement Techniques*, 9(1):159–177, January 2016. ISSN 1867-1381. doi: 10.5194/amt-9-159-2016. URL https://amt.copernicus.org/articles/9/159/2016/. Publisher: Copernicus GmbH.

Dragos A. Vas, Steven E. Peckham, Carl G. Schmitt, Martin Stuefer, Ross G. Burgener, and Telayna E. Wong. Ice fog monitoring near Fairbanks, AK. Report, Cold Regions Research and Engineering Laboratory (U.S.), March 2021. URL https://erdc-library.erdc.dren.mil/jspui/handle/11681/40019. Accepted: 2021-03-19T13:24:30Z Artwork Medium: PDF/A Interview Medium: PDF/A Publication Title: This Digital Resource was created in Microsoft Word and Adobe Acrobat.

I. Gultepe, B. Zhou, J. Milbrandt, A. Bott, Y. Li, A. J. Heymsfield, B. Ferrier, R. Ware, M. Pavolonis, T. Kuhn, J. Gurka, P. Liu, and J. Cermak. A review on ice fog measurements and

modeling. *Atmospheric Research*, 151:2–19, January 2015. ISSN 0169-8095. doi: 10.1016/j.atmosres.2014.04.014. URL https://www.sciencedirect.com/science/article/pii/S0169809514001963.

Katsuhiro Kikuchi. Observation of Cloud Condensation Nuclei at Syowa Station, Antarctica. *Journal of the Meteorological Society of Japan. Ser. II*, 49(5):376–383, 1971a. ISSN 0026-1165, 2186-9057. doi: 10.2151/jmsj1965.49.5_376. URL https://www.jstage.jst.go.jp/article/jmsj1965/49/5/49_5_376/_article/-char/ja/. Publisher: Meteorological Society of Japan.

Katsuhiro Kikuchi. Observations of Concentration of Ice Nuclei at Syowa Station, Antarctica. *Journal of the Meteorological Society of Japan. Ser. II*, 49(1):20–31, 1971b. ISSN 0026-1165, 2186-9057. doi: 10.2151/jmsj1965.49.1_20. URL https://www.jstage.jst.go.jp/article/jmsj1965/49/1/49_1_20/_article/-char/ja/. Publisher: Meteorological Society of Japan.

Katsuhiro Kikuchi. Sintering Phenomenon of Frozen Cloud Particles Observed at Syowa Station, Antarctica. *Journal of the Meteorological Society of Japan. Ser. II*, 50(2):131–135, 1972. ISSN 0026-1165, 2186-9057. doi: 10.2151/jmsj1965.50.2_131. URL https://www.jstage.jst.go.jp/article/jmsj1965/50/2/50_2_131/_article/-char/ja/. Publisher: Meteorological Society of Japan.

Xuwu Chen, Xiaodong Li, Xingzhong Yuan, Guangming Zeng, Jie Liang, Xin Li, Wanjun Xu, Yuan Luo, and Gaojie Chen. Effects of human activities and climate change on the reduction of visibility in Beijing over the past 36years. *Environment International*, 116:92–100, July 2018. ISSN 1873-6750. doi: 10.1016/j.envint.2018.04.009.

Cuiqi Zhang, Zhijun Wu, Jingchuan Chen, Jie Chen, Lizi Tang, Wenfei Zhu, Xiangyu Pei, Shiyi Chen, Ping Tian, Song Guo, Limin Zeng, Min Hu, and Zamin A. Kanji. Ice-nucleating particles from multiple aerosol sources in the urban environment of Beijing under mixed-phase cloud conditions. *Atmospheric Chemistry and Physics*, 22(11):7539–7556, June 2022. ISSN 1680-7316. doi: 10.5194/acp-22-7539-2022. URL https://acp.copernicus.org/articles/22/7539/2022/. Publisher: Copernicus GmbH.

Randolph D. Borys. Studies of ice nucleation by Arctic aerosol on AGASP-II. *Journal of Atmospheric Chemistry*, 9(1):169–185, July 1989. ISSN 1573-0662. doi: 10.1007/BF00052831. URL https://doi.org/10.1007/BF00052831.

Bin Zhao, Yuan Wang, Yu Gu, Kuo-Nan Liou, Jonathan H. Jiang, Jiwen Fan, Xiaohong Liu, Lei Huang, and Yuk L. Yung. Ice nucleation by aerosols from anthropogenic pollution. *Nature Geoscience*, 12(8):602–607, August 2019. ISSN 1752-0908. doi: 10.1038/s41561-019-0389-4. URL https://www.nature.com/articles/s41561-019-0389-4. Number: 8 Publisher: Nature Publishing Group.

Larissa Lacher, Martin Steinbacher, Nicolas Bukowiecki, Erik Herrmann, Assaf Zipori, and Zamin A. Kanji. Impact of Air Mass Conditions and Aerosol Properties on Ice Nucleating Particle Concentrations at the High Altitude Research Station Jungfraujoch. *Atmosphere*, 9(9): 363, 2018. ISSN 2073-4433. doi: 10.3390/atmos9090363. URL

https://www.mdpi.com/2073-4433/9/9/363. Number: 9 Publisher: Multidisciplinary Digital Publishing Institute.

Jann Schrod, Erik S. Thomson, Daniel Weber, Jens Kossmann, Christopher Pöhlker, Jorge Saturno, Florian Ditas, Paulo Artaxo, Valérie Clouard, Jean-Marie Saurel, Martin Ebert, Joachim Curtius, and Heinz G. Bingemer. Long-term deposition and condensation ice-nucleating particle measurements from four stations across the globe. *Atmospheric Chemistry and Physics*, 20(24): 15983–16006, December 2020. ISSN 1680-7316. doi: 10.5194/acp-20-15983-2020. URL https://acp.copernicus.org/articles/20/15983/2020/. Publisher: Copernicus GmbH.

Heike Wex, Lin Huang, Wendy Zhang, Hayley Hung, Rita Traversi, Silvia Becagli, Rebecca J. Sheesley, Claire E. Moffett, Tate E. Barrett, Rossana Bossi, Henrik Skov, Anja Hünerbein, Jasmin Lubitz, Mareike Löffler, Olivia Linke, Markus Hartmann, Paul Herenz, and Frank Stratmann. Annual variability of ice-nucleating particle concentrations at different Arctic locations. *Atmospheric Chemistry and Physics*, 19(7):5293–5311, April 2019. ISSN 1680-7316. doi: 10.5194/acp-19-5293-2019. URL https://acp.copernicus.org/articles/19/5293/2019/. Publisher: Copernicus GmbH.

Naama Reicher, Carsten Budke, Lukas Eickhoff, Shira Raveh-Rubin, Ifat Kaplan-Ashiri, Thomas Koop, and Yinon Rudich. Size-dependent ice nucleation by airborne particles during dust events in the eastern Mediterranean. *Atmospheric Chemistry and Physics*, 19(17):11143–11158, September 2019. ISSN 1680-7316. doi: 10.5194/acp-19-11143-2019. URL https://acp.copernicus.org/articles/19/11143/2019/. Publisher: Copernicus GmbH.

Jingchuan Chen, Zhijun Wu, Jie Chen, Naama Reicher, Xin Fang, Yinon Rudich, and Min Hu. Size-resolved atmospheric ice-nucleating particles during East Asian dust events. *Atmospheric Chemistry and Physics*, 21(5):3491–3506, March 2021. ISSN 1680-7316. doi: 10.5194/acp-21-3491-2021. URL https://acp.copernicus.org/articles/21/3491/2021/. Publisher: Copernicus GmbH.

R. H. Mason, M. Si, C. Chou, V. E. Irish, R. Dickie, P. Elizondo, R. Wong, M. Brintnell, M. Elsasser, W. M. Lassar, K. M. Pierce, W. R. Leaitch, A. M. MacDonald, A. Platt, D. Toom-Sauntry, R. Sarda-Estève, C. L. Schiller, K. J. Suski, T. C. J. Hill, J. P. D. Abbatt, J. A. Huffman, P. J. DeMott, and A. K. Bertram. Size-resolved measurements of ice-nucleating particles at six locations in North America and one in Europe. *Atmospheric Chemistry and Physics*, 16(3):1637–1651, February 2016. ISSN 1680-7316. doi: 10.5194/acp-16-1637-2016. URL https://acp.copernicus.org/articles/16/1637/2016/. Publisher: Copernicus GmbH.

Baptiste Testa, Thomas C. J. Hill, Nicholas A. Marsden, Kevin R. Barry, Carson C. Hume, Qijing Bian, Jun Uetake, Hannah Hare, Russell J. Perkins, Ottmar Möhler, Sonia M. Kreidenweis, and Paul J. DeMott. Ice Nucleating Particle Connections to Regional Argentinian Land Surface Emissions and Weather During the Cloud, Aerosol, and Complex Terrain Interactions Experiment. *Journal of Geophysical Research: Atmospheres*, 126(23):e2021JD035186, 2021. ISSN 2169-8996. doi: 10.1029/2021JD035186. URL https://agupubs.onlinelibrary.wiley.com/doi/full/10.1029/2021JD035186. _eprint: https://onlinelibrary.wiley.com/doi/pdf/10.1029/2021JD035186.

K. A. Koehler, S. M. Kreidenweis, P. J. DeMott, M. D. Petters, A. J. Prenni, and O. Möhler. Laboratory investigations of the impact of mineral dust aerosol on cold cloud formation. *Atmospheric Chemistry and Physics*, 10(23):11955–11968, December 2010. ISSN 1680-7316. doi: 10.5194/acp-10-11955-2010. URL https://acp.copernicus.org/articles/10/11955/2010/. Publisher: Copernicus GmbH.

Kevin R. Barry, Thomas C. J. Hill, Kathryn A. Moore, Thomas A. Douglas, Sonia M. Kreidenweis, Paul J. DeMott, and Jessie M. Creamean. Persistence and Potential Atmospheric Ramifications of Ice-Nucleating Particles Released from Thawing Permafrost. *Environmental Science & Technology*, 57(9):3505–3515, March 2023. ISSN 0013-936X. doi: 10.1021/acs.est.2c06530. URL https://doi.org/10.1021/acs.est.2c06530. Publisher: American Chemical Society.

Jessie M. Creamean, Thomas C. J. Hill, Paul J. DeMott, Jun Uetake, Sonia Kreidenweis, and Thomas A. Douglas. Thawing permafrost: an overlooked source of seeds for Arctic cloud formation. *Environmental Research Letters*, 15(8):084022, July 2020. ISSN 1748-9326. doi: 10.1088/1748-9326/ab87d3. URL https://dx.doi.org/10.1088/1748-9326/ab87d3. Publisher: IOP Publishing.

Gregory P. Schill, Paul J. DeMott, Ethan W. Emerson, Anne Marie C. Rauker, John K. Kodros, Kaitlyn J. Suski, Thomas C. J. Hill, Ezra J. T. Levin, Jeffrey R. Pierce, Delphine K. Farmer, and Sonia M. Kreidenweis. The contribution of black carbon to global ice nucleating particle concentrations relevant to mixed-phase clouds. *Proceedings of the National Academy of Sciences*, 117(37):22705–22711, September 2020. doi: 10.1073/pnas.2001674117. URL https://www.pnas.org/doi/full/10.1073/pnas.2001674117. Publisher: Proceedings of the National Academy of Sciences.

Kevin R. Barry, Thomas C. J. Hill, Ezra J. T. Levin, Cynthia H. Twohy, Kathryn A. Moore, Zachary D. Weller, Darin W. Toohey, Mike Reeves, Teresa Campos, Roy Geiss, Gregory P. Schill, Emily V. Fischer, Sonia M. Kreidenweis, and Paul J. DeMott. Observations of Ice Nucleating Particles in the Free Troposphere From Western US Wildfires. *Journal of Geophysical Research: Atmospheres*, 126(3):e2020JD033752, 2021. ISSN 2169-8996. doi: 10.1029/2020JD033752. URL https://onlinelibrary.wiley.com/doi/abs/10.1029/2020JD033752. _eprint: https://onlinelibrary.wiley.com/doi/pdf/10.1029/2020JD033752.

Martin I. Daily, Mark D. Tarn, Thomas F. Whale, and Benjamin J. Murray. An evaluation of the heat test for the ice-nucleating ability of minerals and biological material. *Atmospheric Measurement Techniques*, 15(8):2635–2665, May 2022. ISSN 1867-1381. doi: 10.5194/amt-15-2635-2022. URL https://amt.copernicus.org/articles/15/2635/2022/. Publisher: Copernicus GmbH.

B. R. T. Simoneit, J. J. Schauer, C. G. Nolte, D. R. Oros, V. O. Elias, M. P. Fraser, W. F. Rogge, and G. R. Cass. Levoglucosan, a tracer for cellulose in biomass burning and atmospheric particles. *Atmospheric Environment*, 33(2):173–182, January 1999. ISSN 1352-2310. doi: 10.1016/S1352-2310(98)00145-9. URL https://www.sciencedirect.com/science/article/pii/S1352231098001459.

Md. Mozammel Haque, Kimitaka Kawamura, Dhananjay K. Deshmukh, Bhagawati Kunwar, and Yongwon Kim. Biomass Burning is an Important Source of Organic Aerosols in Interior Alaska.

Journal of Geophysical Research: Atmospheres, 126(12):e2021JD034586, 2021. ISSN 2169-8996. doi: 10.1029/2021JD034586. URL https://onlinelibrary.wiley.com/doi/abs/10.1029/2021JD034586. _eprint: https://onlinelibrary.wiley.com/doi/pdf/10.1029/2021JD034586.

Lea Hartl, Carl Schmitt, Telayna Wong, Dragos A. Vas, Lewis Enterkin, and Martin Stuefer. Long-Term Trends in Ice Fog Occurrence in the Fairbanks, Alaska, Region Based on Airport Observations. *Journal of Applied Meteorology and Climatology*, 62(9):1263–1278, September 2023. ISSN 1558-8424, 1558-8432. doi: 10.1175/JAMC-D-22-0190.1. URL https://journals.ametsoc.org/view/journals/apme/62/9/JAMC-D-22-0190.1.xml. Publisher: American Meteorological Society Section: Journal of Applied Meteorology and Climatology.

P. J. DeMott, A. J. Prenni, G. R. McMeeking, R. C. Sullivan, M. D. Petters, Y. Tobo, M. Niemand, O. Möhler, J. R. Snider, Z. Wang, and S. M. Kreidenweis. Integrating laboratory and field data to quantify the immersion freezing ice nucleation activity of mineral dust particles. *Atmospheric Chemistry and Physics*, 15(1):393–409, January 2015. ISSN 1680-7316. doi: 10.5194/acp-15-393-2015. URL https://acp.copernicus.org/articles/15/393/2015/. Publisher: Copernicus GmbH.

E. V. Fischer, K. D. Perry, and D. A. Jaffe. Optical and chemical properties of aerosols transported to Mount Bachelor during spring 2010. *Journal of Geophysical Research: Atmospheres*, 116 (D18), 2011. ISSN 2156-2202. doi: 10.1029/2011JD015932. URL https://onlinelibrary.wiley.com/doi/abs/10.1029/2011JD015932. _eprint: https://onlinelibrary.wiley.com/doi/pdf/10.1029/2011JD015932.

Appendix A

ADDITIONAL TABLES AND FIGURES

Table A.1: Metadata for DRUM samples, including collection dates and times. The stages that were subject to INP processing are indicated by a checkmark.

Start Datetime (AKST)	End Datetime (AKST)	3-12 µm Processing	1.2-3 µm Processing	0.3-1.2 µm Processing	0.15-0.3 µm Processing
1/17/22 9:00	1/18/22 9:00				
1/18/22 9:00	1/19/22 9:24				
1/19/22 9:24	1/20/22 9:06				
1/20/22 9:06	1/21/22 9:18				
1/21/22 9:18	1/22/22 9:01				
1/22/22 9:01	1/23/22 8:57				
1/23/22 8:57	1/24/22 9:11				
1/24/22 9:11	1/25/22 8:56				
1/25/22 8:56	1/26/22 9:11				
1/26/22 9:11	1/27/22 8:54				
1/27/22 8:54	1/28/22 8:54				
1/28/22 8:54	1/29/22 9:00				
1/29/22 9:00	1/29/22 21:00				
1/29/22 21:00	1/30/22 8:58	✓			✓
1/30/22 8:58	1/30/22 21:31				
1/30/22 21:31	1/31/22 9:13				
1/31/22 9:13	1/31/22 20:28				
1/31/22 20:28	2/1/22 8:59				
2/1/22 8:59	2/1/22 20:50				

Start Datetime (AKST)	End Datetime (AKST)	3-12 µm Processing	1.2-3 µm Processing	0.3-1.2 µm Processing	0.15-0.3 µm Processing
2/1/22 20:50	2/2/22 9:05				
2/2/22 9:05	2/2/22 20:54				
2/2/22 20:54	2/3/22 9:04	✓			✓
2/3/22 9:04	2/3/22 21:51				
2/3/22 21:51	2/4/22 8:58				
2/4/22 8:58	2/4/22 9:17				
2/4/22 9:17	2/5/22 8:57				
2/5/22 8:57	2/6/22 9:00				
2/6/22 9:00	2/7/22 9:10				
2/7/22 9:10	2/8/22 9:04				
2/8/22 9:04	2/9/22 9:02				
2/9/22 9:02	2/10/22 9:04				
2/10/22 9:04	2/11/22 9:02				
2/11/22 9:02	2/12/22 8:59				
2/12/22 8:59	2/13/22 8:58				
2/13/22 8:58	2/14/22 9:03				
2/14/22 9:03	2/15/22 9:02				
2/15/22 9:02	2/16/22 9:03				
2/16/22 9:03	2/17/11 9:19				
2/17/11 9:19	2/17/11 14:11				
2/17/11 14:11	2/18/22 9:00				
2/18/22 9:00	2/19/22 8:58	✓			✓
2/19/22 8:58	2/20/22 8:53				
2/20/22 8:53	2/21/22 9:07				

Start Datetime (AKST)	End Datetime (AKST)	3-12 µm Processing	1.2-3 µm Processing	0.3-1.2 µm Processing	0.15-0.3 µm Processing
2/21/22 9:07	2/22/22 9:00				
2/22/22 9:00	2/23/22 9:08				
2/23/22 9:08	2/24/22 9:58				
2/24/22 9:58	2/25/22 8:51	✓			✓
2/25/22 8:51	2/26/22 9:00				

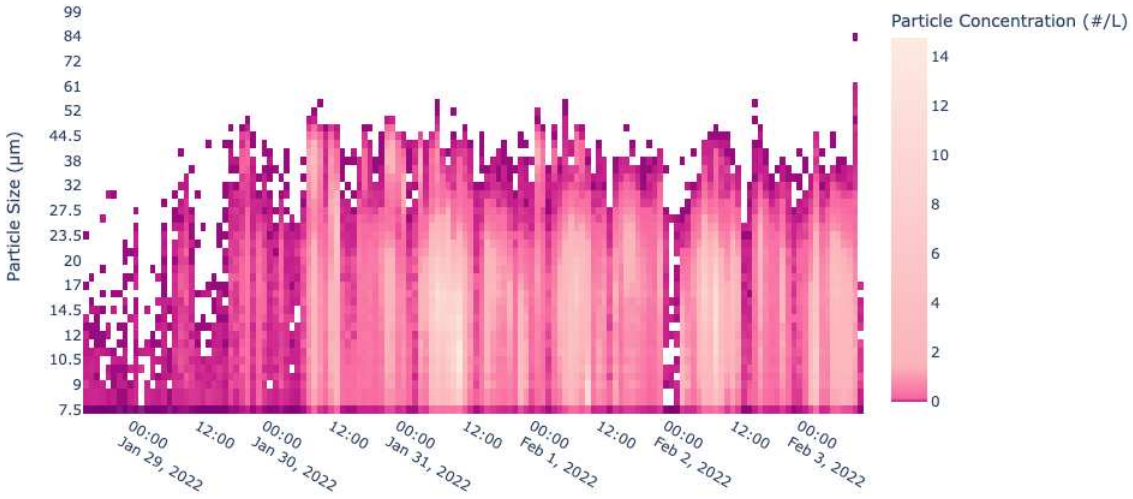

Figure A.1: Ice crystal concentrations at Fort Wainwright during the ice fog period. For the entire segment, liquid droplets were 0.75% and ice crystals were 99.25% of the total particles measured.

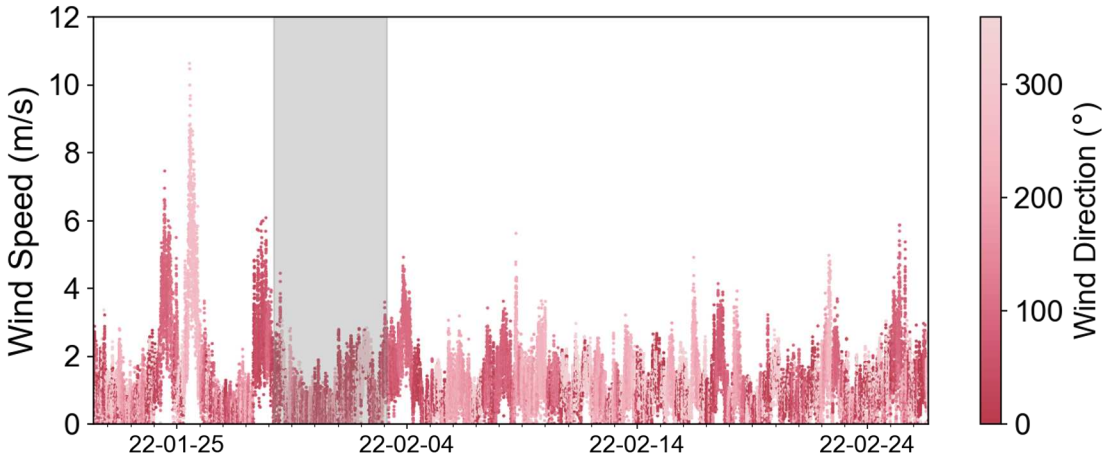

Figure A.2: Time series of wind speed, colored by wind direction. The ice fog period is denoted by gray shading.

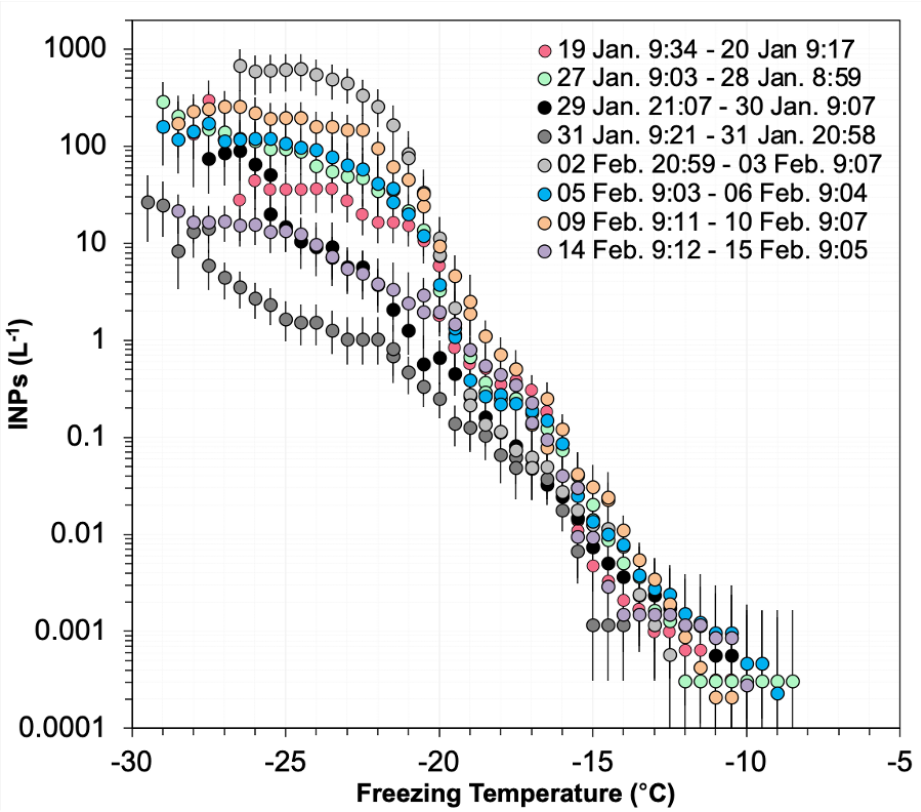

Figure A.3: Cumulative total INP spectra for filters that were selected for treatments. The gray/black colors indicate filters from the ice fog period.

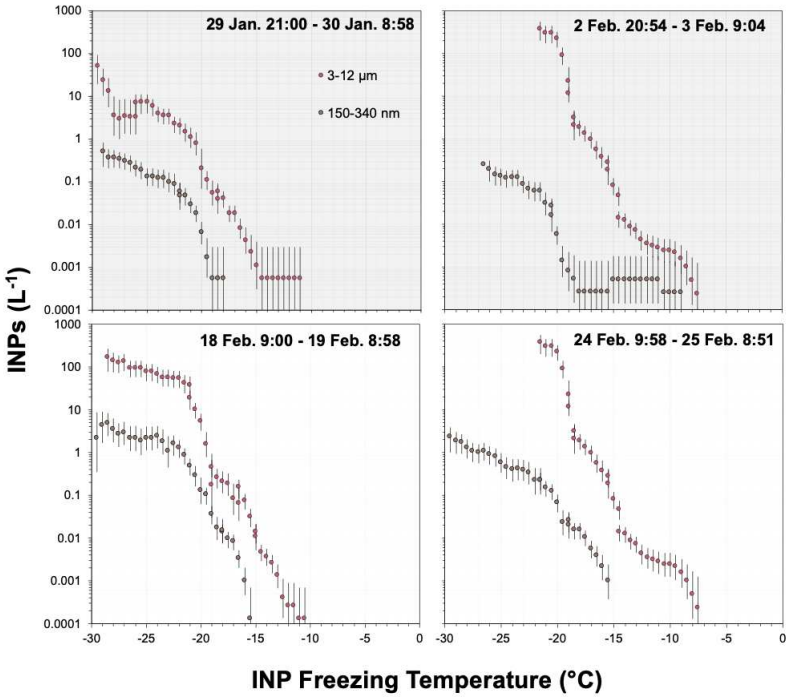

Figure A.4: Cumulative INP spectra 150-340 nm and 3-12 µm DRUM size bins.

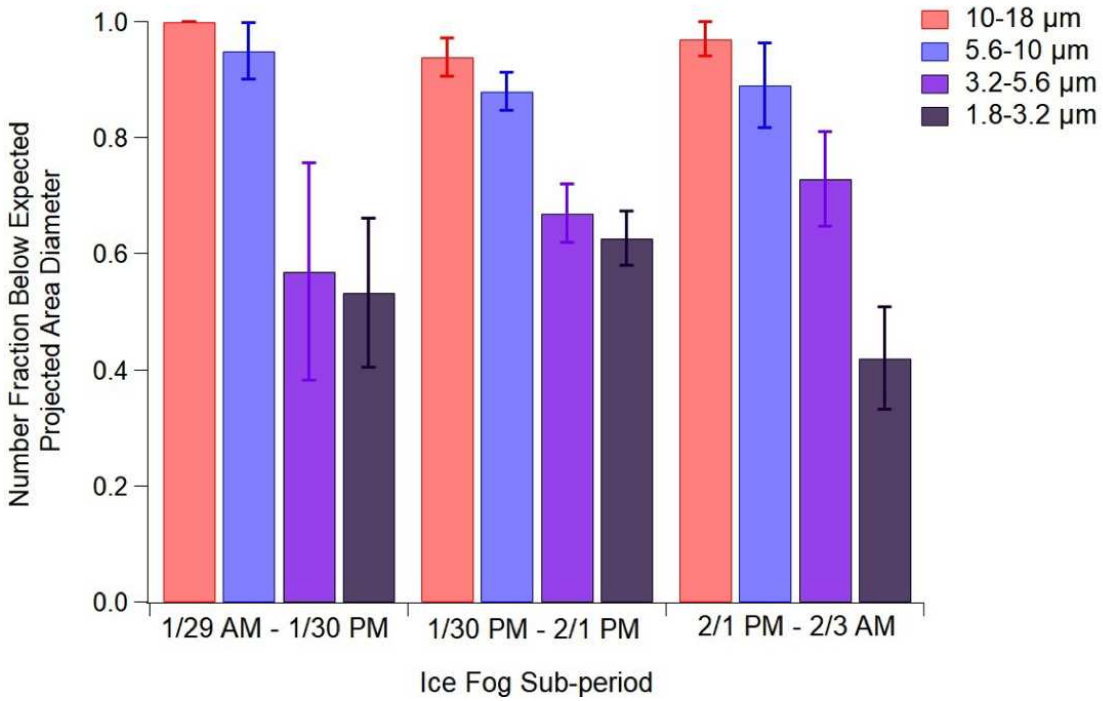

Figure A.5: Number fraction of particles below expected area diameter on different MOUDI stages during the ice fog subperiods.

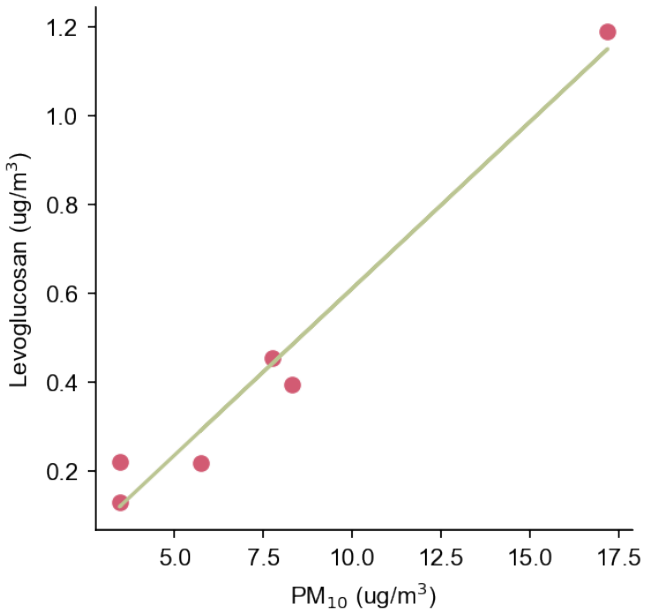

Figure A.6: Scatter plot of levoglucosan measured from select filters and total PM_{10} mass concentrations.

A.1 PRINCIPAL COMPONENT ANALYSIS

We used empirical orthogonal function (EOF) analysis to understand variability in PM_{10} metal composition. EOF analysis explains the variance in a dataset by decomposing the data into mathematically independent structures. The data was normalized, then decomposed into eigenvalues and eigenvectors (EOFs) which were projected onto the original data, resulting in the principal components. In this study, the principal components are representative of metal composition patterns, while the principal components are indicative of the time dimension. The magnitude of the eigenvalues represent how much of the data is explained by each EOF.

Our EOF analysis of XRF data shows that principal component 1 (PC1) explains over 80% of the variance in the data. PC1 peaks during ice fog periods 1 and 2. EOF 1 mostly comprised of sulfur but also contains some potassium, calcium, iron, and zinc. This EOF is likely indicative of dust with sulfate. The combination of Ca and S demonstrates that the dust is partnered with combustion (Fischer et al., 2011). A dust signature peaking during the ice fog period is consistent with our filter treatment results as the percentage of inorganic INPs is highest during the ice fog

period. Our EOF analysis is also consistent with the large dust fraction that was seen in the single particle composition analysis.

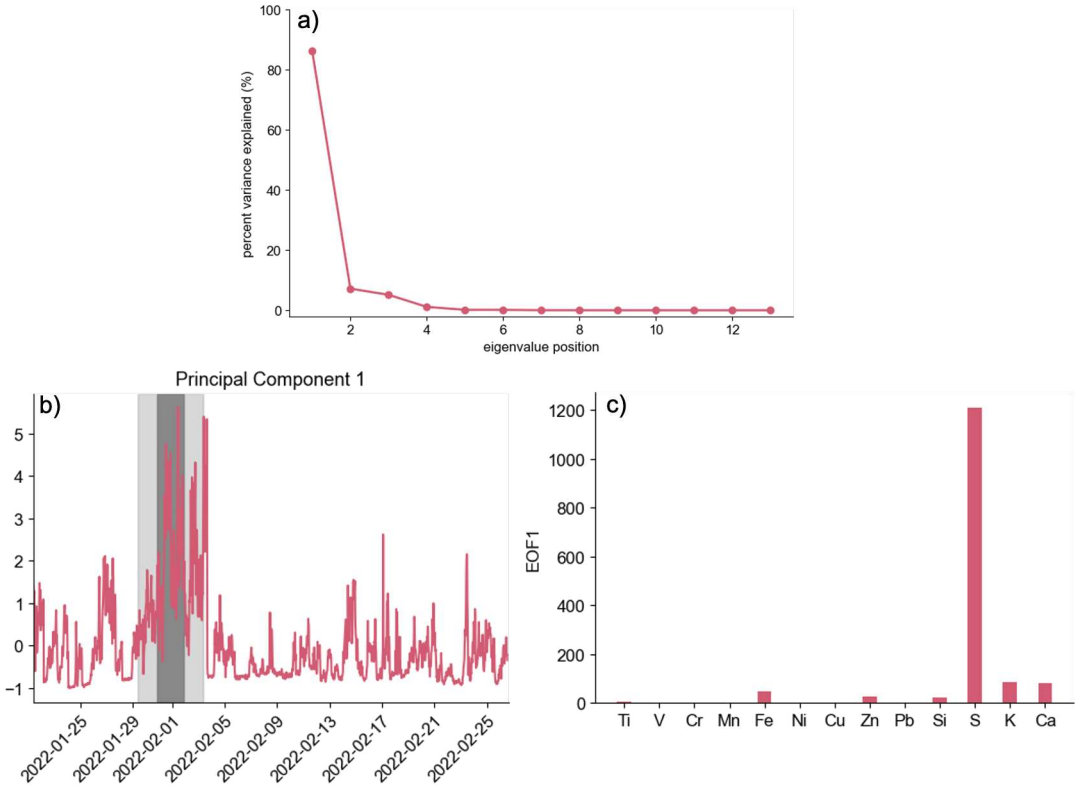

Figure A.7: a) Percent variance explained by each EOF. b) Timeseries of principal component 1 with the ice fog sub periods indicated in grey. c) Components of principal component 1.